BSc thesis APPLIED MATHEMATICS & APPLIED PHYSICS

"Synchronisation of systems containing four coupled quantum van der Pol oscillators"

Wiggert Vermeer
5011620

Delft University of Technology

Supervisors

Dr. J. L. A. Dubbeldam Prof. Dr. Y. M. Blanter

Committee members

Dr J. G. Spandaw Dr. J. M. Thijssen

August, 2022 Delft

Abstract

Synchronisation refers to the tendency of coupled oscillators to move in phase with one another over time, departing from their own natural frequency. This phenomenon occurs in almost all branches of science, engineering, and social life. Synchronisation is a well understood concept in classical mechanics. Quantum synchronisation involves attempting to extend this concept to quantum mechanics, where there are number of phenomena such as damping that are more difficult to realise. This thesis focuses on two things. Firstly, it explores the bridge between classical and quantum synchronisation. Both the equivalencies as well as the difficulties that must be overcome. This is initially done by looking at a simple classical model for two coupled oscillators and extending this to a quantum model, and subsequently by exploring the derivation of a master equation for a damped quantum harmonic oscillator with non-linear damping. Secondly, it explore the synchronisation of four coupled quantum van der Pol oscillators. To this purpose, the six different systems (tree, chain, loop, tower, spade, all-to-all) with four coupled classical van der Pol oscillators first analysed and the Arnold tongues are determined, showing for what parameters synchronisation is expected to occur. The equivalent systems with four quantum van der Pol oscillators are explored to determine whether the classical Arnold tongues give a good indication of when quantum synchronisation is expected to occur. An alternative measure for synchronisation is also investigated for these systems based on the relative entropy of coherence. The Arnold tongues for each of the four classical oscillator systems were determined. For some systems (chain and loop) the Arnold tongues were much smaller than for the three oscillator system while for others (tree, all-to-all) they were only slightly smaller. The quantum Arnold tongues showed very similar behaviour to the classical Arnold tongues. Furthermore, when investigating the correlations between different pairs of oscillators, it was found that the correlation decreased as the number of connections separating two oscillators increased. In the chain system, an expected symmetry was found. The relative entropy of coherence is found to be a good measure of synchronisation, better than the more frequently used complex correlator. This is because the relative entropy can take into account the entire system, while the correlator describes the synchronisation between two individual oscillators in the system.

Contents

1

Introduction

Synchronisation refers to a variety of phenomena and occurs in almost all branches of science, engineering and social life. It means "to occur in the same time", and the essence of synchronisation is the adjustment of rhythm due to an interaction. Classical harmonic oscillators with different natural frequencies can be coupled to one another in order to oscillate at a new frequency. This phenomenon was first observed by Christaan Huygens in the 17th century, when pendulum clocks aboard a ship would eventually have their oscillations coincide with one another [1].

Quantum synchronisation refers to the synchronisation of oscillators in the quantum limit. There are a number of features of quantum systems which will affect how such systems can be related to classical systems: The discrete nature of quantum systems, the concept of superposition, and the incorporation of damping. Applications of quantum synchronisation include the synchronisation of spins in a quantum magnet which has the potential to improve the resolution of MRI images, and it could play a role in quantum key distribution [2].

This thesis will focus on the synchronisation of quantum van der Pol oscillators. Synchronisation of quantum van der Pol oscillators has previously been explored in environments with an external drive and reactive coupling between two, and infinitely many coupled oscillators [3], dissipative coupling between two and many coupled oscillators [4] and three coupled oscillators [5]. This thesis will build upon the work done in [5] and focus on systems with 4 coupled quantum van der Pol oscillators. There are 6 ways to set up the coupling between 4 (identical) oscillators, each of which will be investigated in both the classical and the quantum case.

Chapter 2 begins with the discussion of a simple classical model where synchronisation can occur, which in Chapter 4 will be extended to the quantum case. Subsequently the classical van der Pol oscillator will be discussed. The conditions for synchronisation to be possible will be determined for systems of two-, three-, and four- coupled classical van der Pol oscillators. Chapter 3 will discuss a number of quantum preliminaries needed to understand the quantum van der Pol oscillator. First the difficulties of incorporating damping into a quantum system will be laid out, followed by a derivation of master equations for damped quantum harmonic oscillators . Chapter 4 looks at quantum synchronisation and consists of two sections. First it extends the discrete classical model presented in Chapter 1 and investigates the synchronisation behaviour in this quantum model. Second, it discusses how the synchronisation of quantum van der Pol oscillators will be investigated, with an emphasis on four oscillator systems. The results for the systems of quantum van der Pol oscillators are presented and discussed in Chapter 5. Chapter 6 gives a conclusion of the results found in the thesis, and proposes avenues for future research.

2

Classical Synchronisation

To understand the key principles of synchronisation, it is useful to consider simple models of coupled oscillators, where the behaviour is more predictable. When these simple classical models are eventually extended to quantum models, the difficulties faced will be more explicit. First the simple models for oscillators described in [6] are considered.

2.1. Simple model

Consider an oscillator moving on a circular domain with angular frequency Ω. Its position can be described by a phase $\theta \in [0, 2\pi)$. On the same circular domain, another oscillator moves with frequency ω, however this oscillator's movement is also impacted by a driving force influenced by the relative position of the two oscillators. This system can be described by the following equations of motion:

$$\dot{\theta} = \Omega \qquad \mod 2\pi, \tag{2.1}$$

$$\dot{\phi} = \omega + Kf(\theta - \phi) \quad \mod 2\pi, \tag{2.2}$$

where $\phi \in [0, 2\pi)$ denotes the phase of the second oscillator, $f : [0, 2\pi) \to \mathbb{R}$ is an arbitrary function of the difference of the two phases of the two oscillators, and K is a measure of the strength of the driving force. The first oscillator will be called the 'stimulus' while the second oscillator will be referred to as simply the 'oscillator'.

The phenomenon of interest is phase locking, which occurs when the stimulus and oscillator move in such a way that their phase difference remains the same, although they are not necessarily stationary. The equation of motion for the phase difference $\Delta = \theta - \phi$ follows from Equations (2.1) and (2.2):

$$\dot{\Delta} = (\Omega - \omega) - Kf(\Delta). \tag{2.3}$$

For phase locking to occur, it is required that $\dot{\Delta}$ can take on the value 0. This means that there must be a value Δ such that $f(\Delta) = \frac{(\Omega-\omega)}{K}$, implying that $\frac{(\Omega-\omega)}{K}$ must lie within the range of f. If this condition is not satisfied, phase locking cannot occur and the stimulus and oscillator will never be synchronised. Figure 2.1 shows an example where synchronisation occurs with this model.

2.2. Discrete model

The model can be adjusted to take place on a discrete circle consisting of d positions, or dimensions. The reason why this is a change of interest is related to the quantisation that takes place in quantum mechanics, where only discrete energy levels, or states, can be occupied. For now, only the classical model will be considered, but later the extension to a quantum model will be discussed. Equations (2.1), (2.2) and (2.3) are modified to be discrete:

$$\theta_{t+1} = \theta_t + \Omega, \tag{2.4}$$

$$\phi_{t+1} = \phi_t + \omega + G_K(\theta_t - \phi_t), \tag{2.5}$$

$$\Delta_{t+1} = \Delta_t + (\Omega - \omega) - G_K(\Delta_t), \tag{2.6}$$

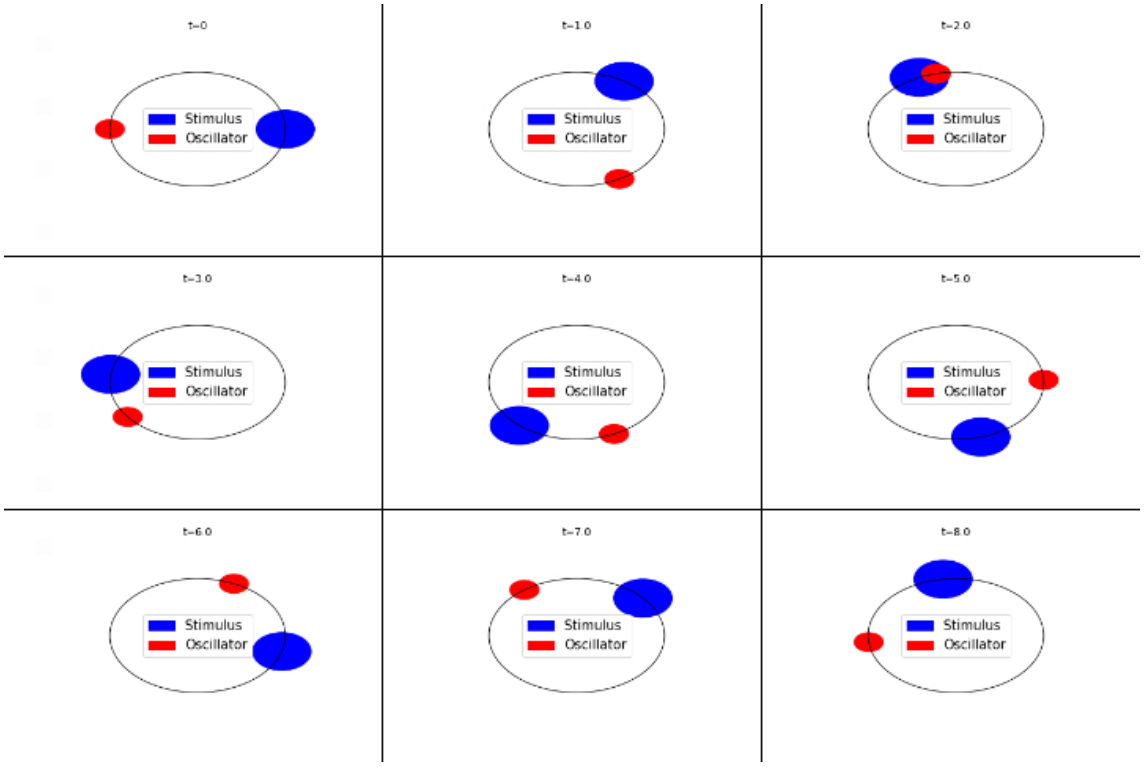

Figure 2.1: Continuous time evolution of a the phases of the stimulus and oscillator found by numerically integrating Equations (2.1), (2.2) and (2.3) with parameters $\Omega = 1$, $\omega = 2$, $K = 1$, $f(\Delta) = \sin(\Delta)$. Both oscillators move along the circular path and the system slowly evolves into the synchronised state where $\Delta = \frac{3\pi}{2}$. This value changes very slowly with time, so at $t = 8$, this Δ has not been reached yet (although it is very close). It is not until $t = 430$ that Δ lies within within 0.1% of $\frac{3\pi}{2}$. Note that the movement is anti-clockwise.

where $G_K(\Delta)$ takes the place of $Kf(\Delta)$. Rather than occuring on a circle such that $\theta_t, \phi_t \in [0, 2\pi)$, they occur in a system with dimension d such that $\theta_t, \phi_t \in \{0, 1, 2, 3, ...d\}$ and all values are taken mod d. Furthermore, Ω, ω and G_K are chosen such that only integer values are allowed. Similar to the continuous model, for phase locking to occur it is required that $\exists t$ s.t $G_K(\Delta_t) = (\Omega - \omega)$.

G_K can be specified such that for a certain range around the position of the stimulus, the oscillator would be forced to the position of the stimulus before they both perform their next rotation:

$$G_K(\Delta_t) = \begin{cases} \Delta_t, & \text{if } |\Delta_t| \leq K, \\ 0, & \text{otherwise,} \end{cases} \tag{2.7}$$

with Δ_t mod d taken such that $|\Delta_t|$ is minimised. This means that the condition for phase locking becomes $|(\Omega - \omega)| \leq K$. Figure 2.2 show the time evolution of such a system where synchronisation occurs after five steps.

This section gives a basic idea of what synchronisation looks like in a system in the form of phase locking. However in the real world, oscillators do not move in such a simple away. In the next section an oscillator that has a physical basis will be discussed, namely the van der Pol oscillator.

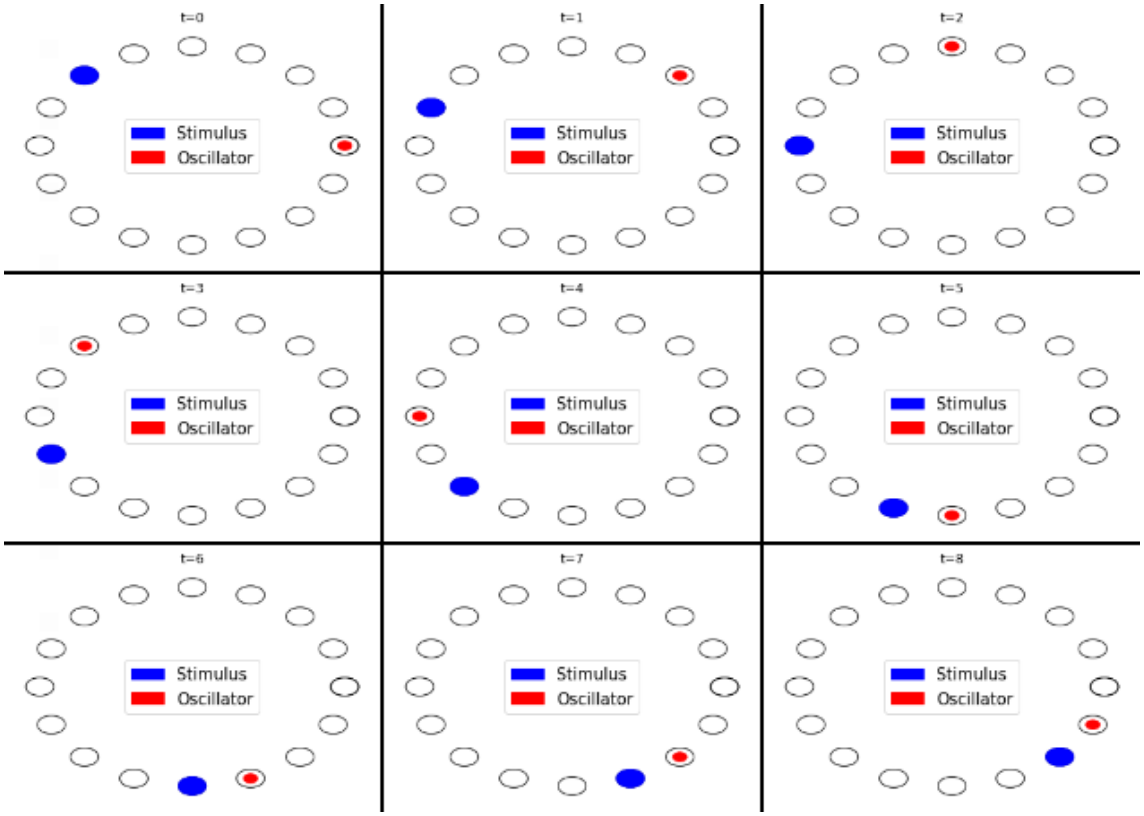

Figure 2.2: Figures showing the discrete time evolution of a stimulus and oscillator found by iterating Equations (2.4), (2.5) and (2.6) with parameters $\Omega = 1$, $\omega = 2$, $K = 2$. The system evolves to the synchronised state when $\Delta = -1 = \Omega - \omega$. Note that the movement is anti-clockwise.

2.3. Classical van der Pol oscillator

The classical van der Pol oscillator has been very well studied in the past century, ever since it was first proposed in 1926. It has the following equation of motion:

$$\ddot{x} - \mu(1 - \beta x^2)\dot{x} + \omega_0^2 x = 0, \tag{2.8}$$

where the notation $\dot{x} = \frac{dx}{dt}$ is used.

Without the second term, this equation takes the form of the simple harmonic oscillator with natural frequency ω_0. The second term represents the damping. The term proportional to β gives non-linear damping, while the other term gives negative linear damping. The result of including these terms, is that there is *dissipation* present in the system. The negative damping allows the oscillator to take energy from a source, while the non-linear damping leads to energy loss, allowing the oscillator to maintain stable oscillatory motion [7].

2.3.1. Amplitude equation

Assuming that μ is small, Equation (2.8) is close to that of a linear oscillator, so we can assume the solution for x has a nearly harmonic form with a certain amplitude, frequency and phase [1]. The solution can be assumed to be of the following form:

$$x(t) = \frac{1}{2}(A(t)e^{i\omega t} + A^*(t)e^{-i\omega t}), \tag{2.9}$$

where A denotes the complex amplitude.

Equation (2.8) can be rewritten as a system of first order differential equations:

$$\dot{x} = y, \tag{2.10}$$

$$\dot{y} = -\omega^2 x + \mu(1 - \beta x^2)\dot{x}, \tag{2.11}$$

and the following solution for y is introduced:

$$y(t) = \frac{1}{2}(i\omega A(t)e^{i\omega t} - i\omega A^*(t)e^{-i\omega t}). \tag{2.12}$$

Solving these equations for A (see A.1 for explicit calculations of the following steps up to Equation (2.14)) leads to

$$\dot{A}(t) = \frac{e^{-i\omega t}}{i\omega}(\mu(1-\beta x^2)\dot{x}). \tag{2.13}$$

Now the assumption that the parameters μ and β are small will be used. When the terms on the r.h.s of Equation (2.13) are expanded, there are terms that are proportional to $e^{\pm ni\omega t}$ with $n \in \mathbb{N}$, and there are terms that do not oscillate. By neglecting all the terms containing fast oscillations, a solvable solution for $A(t)$ can be found. This is called the method of averaging, as it essentially involves averaging the oscillating terms over a period of $T = \frac{2\pi}{\omega}$ [1].

Performing the averaging gives the following equation:

$$\dot{A}(t) = \frac{\mu}{2}A(t) - \frac{\mu\beta}{8}|A(t)|^2 A(t). \tag{2.14}$$

This is the amplitude equation for the classical van der Pol oscillator. The first and second term describe the linear and nonlinear growth/decay. This equation will be be used to create a link between the classical van der Pol oscillator, and the quantum van der Pol oscillator.

Figure 2.3 shows an example of how a van der Pol oscillator progresses into its limit cycle. The limit cycle is the closed trajectory the oscillator spirals into as time tends to infinity. Upon entering the limit cycle, the oscillator will always return to those same points.

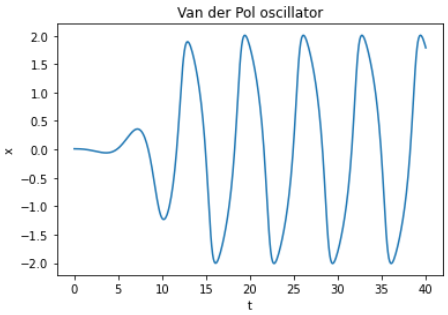

(a) Plot of how the position of a van der Pol oscillator changes in time. At approximately t=12 it has entered a limit cycle.

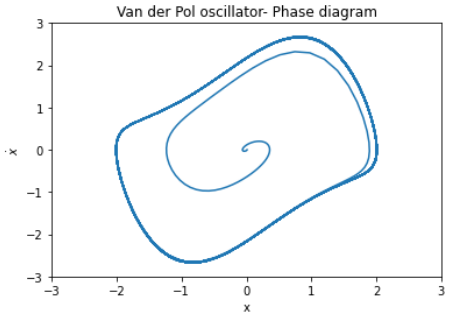

(b) Phase diagram of a van der Pol oscillator, showing how the position and velocity change with respect to one another. The bolder line indicates the limit cycle which the oscillator enters

Figure 2.3: Progression of a van der Pol oscillator described by Equation (2.8) with $\mu = 1, \beta = 1, \omega = 1$ and initial values $x_0 = 0.01, \dot{x}_0 = 0$.

2.4. Two coupled van der Pol oscillators

Two van der Pol oscillators will now be linearly coupled to one another. Their damping rates are kept the same, however the natural frequencies are not necessarily the same. The equations of motion of the two oscillators take the form of:

$$\ddot{x}_1 - \mu(1-\beta x_1^2)\dot{x}_1 + \omega_1^2 x_1 = R(x_2 - x_1) + D(\dot{x}_2 - \dot{x}_1), \tag{2.15}$$

$$\ddot{x}_2 - \mu(1-\beta x_2^2)\dot{x}_2 + \omega_2^2 x_2 = R(x_1 - x_2) + D(\dot{x}_1 - \dot{x}_2). \tag{2.16}$$

Two forms of coupling are present. The term involving R refers to *reactive* coupling and is proportional to the difference in the positions of the two oscillators. The term involving D refers to *dissipative* coupling and is proportional the difference in the velocities. This thesis will focus dissipative coupling so $R = 0$. This enables

comparisons between dissipative coupling in two classical van der Pol oscillators, and dissipative coupling in two quantum van der Pol oscillators.

The addition of these dissipative coupling terms leads to the following amplitude equations:

$$\dot{A_1} = -i\Omega_1 A_1 + \frac{\mu}{2}A_1 - \frac{\mu\beta}{8}|A_1|^2 A_1 + \frac{D}{2}(A_2 - A_1), \tag{2.17}$$

$$\dot{A_2} = -i\Omega_2 A_2 + \frac{\mu}{2}A_2 - \frac{\mu\beta}{8}|A_2|^2 A_2 + \frac{D}{2}(A_1 - A_2), \tag{2.18}$$

where $\Omega_{1,2} = \omega_{1,2} - \omega$ with ω being the frequency used in the ansatz, Equation (2.9). Note that originally the ansatz used the natural frequency of the oscillator for ω, however here a different (unknown) frequency ω is selected for the ansatz in Equation (2.9).

These equations can be written in complex amplitude-argument form allowing the phase difference between the two oscillators to be studied. By introducing $A_{1,2} = r_{1,2}e^{i\phi_{1,2}}$, the system of equations becomes

$$\dot{r_1} = \frac{\mu}{2}r_1 - \frac{\mu\beta}{8}r_1^3 + \frac{D}{2}(-r_1 + r_2\cos(\phi_2 - \phi_1)), \tag{2.19}$$

$$\dot{r_2} = \frac{\mu}{2}r_2 - \frac{\mu\beta}{8}r_2^3 + \frac{D}{2}(-r_2 + r_1\cos(\phi_1 - \phi_2)), \tag{2.20}$$

$$\dot{\phi_1} = -\Omega_1 + \frac{D}{2}\frac{r_2}{r_1}\sin(\phi_2 - \phi_1), \tag{2.21}$$

$$\dot{\phi_2} = -\Omega_2 + \frac{D}{2}\frac{r_1}{r_2}\sin(\phi_1 - \phi_2). \tag{2.22}$$

$$\tag{2.23}$$

Then the phase difference $\theta = \phi_2 - \phi_1$ can expressed as:

$$\dot{\theta} = -\Delta_{2,1} - \frac{D}{2}\left(\frac{r_1}{r_2} + \frac{r_2}{r_1}\right)\sin(\theta), \tag{2.24}$$

where $\Delta_{2,1} = \Omega_2 - \Omega_1$.

When the oscillators are uncoupled, they both have a limit cycle with $r_{1,2} = \frac{2}{\sqrt{\beta}}$. Assuming small coupling (but not 0), the dynamics of $r_{1,2}$ can be neglected in which case

$$\dot{\theta} = -\Delta_{2,1} - D\sin(\theta). \tag{2.25}$$

Synchronisation occurs when the phase difference between the two oscillators is constant, i.e $\dot{\theta} = 0$. This occurs when $\sin(\theta) = \Delta_{2,1}/D$. However because the range of $\sin(\theta)$ is bounded, this is not always possible. Synchronisation is only possible if

$$\left|\frac{\Delta_{2,1}}{D}\right| \leq 1. \tag{2.26}$$

Figure 2.4 shows examples of the progression of two van der Pol oscillators. In Figure 2.4a, the coupling is weak so synchronisation does not occur while in Figure 2.4b the coupling is strong enough such that synchronisation does occur.

For systems with more than two oscillators, there are different ways in which the system can be set up in terms of coupling, and bounds similar to Equation (2.26) can be found. These bounds represent regions where synchronisation can occur and are called Arnold tongues [4].

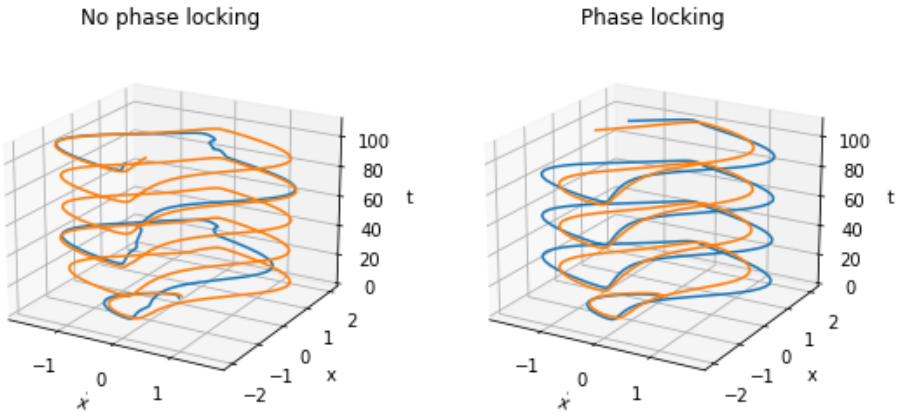

(a) Synchronisation does not occur as $D = 0.1$.

(b) Synchronisation does occur as $D = 1$.

Figure 2.4: Progression of two coupled van der Pol oscillators with parameters $\mu = \beta = 1$, $\omega_1 = 0.2$ and $\omega_2 = 0.4$. For these parameters it is expected that synchronisation occurs if $|D| \geq 0.2$. The system in Figure 2.4b satisfies this bound so synchronisation does occur, while the system in Figure 2.4a does not, so synchronisation does not occur.

2.5. Three coupled van der Pol oscillators

For three oscillators, they can either all be coupled to one another, or one connection can be removed such that there is chain of coupled oscillators. Later in the thesis the focus will be on four oscillator systems of which there are six possible ways of coupling. Three oscillator systems were previously studied in [5] and the synchronisation regimes for those systems are included here such that comparisons can be made to the other systems.

2.5.1. Synchronisation of three all-to-all coupled van der Pol oscillators

Three van der Pol oscillators that are each dissipatively coupled to one another have the following equations for their phase (assuming weak coupling such that $r_i / r_j = 1$):

$$\dot{\phi}_1 = -\Omega_1 + \frac{D}{2}\left(\sin(\phi_2 - \phi_1) + \sin(\phi_3 - \phi_1)\right), \tag{2.27}$$

$$\dot{\phi}_2 = -\Omega_2 + \frac{D}{2}\left(\sin(\phi_1 - \phi_2) + \sin(\phi_3 - \phi_2)\right), \tag{2.28}$$

$$\dot{\phi}_3 = -\Omega_3 + \frac{D}{2}\left(\sin(\phi_1 - \phi_3) + \sin(\phi_2 - \phi_3)\right). \tag{2.29}$$

Writing the phase differences as $\theta_{i,j} = \phi_i - \phi_j$ leads to

$$\dot{\theta}_{2,1} = -\Delta_{2,1} + \frac{D}{2}\left(-2\sin(\theta_{2,1}) + \sin(\theta_{3,2}) - \sin(\theta_{3,2} + \theta_{2,1})\right), \tag{2.30}$$

$$\dot{\theta}_{3,2} = -\Delta_{3,2} + \frac{D}{2}\left(-2\sin(\theta_{3,2}) + \sin(\theta_{2,1}) - \sin(\theta_{3,2} + \theta_{2,1})\right). \tag{2.31}$$

The goal is to find a bound for Δ/D such that for every combination of $\Delta_{1,2}/D$ and $\Delta_{2,3}/D$ chosen within that bound synchronisation is possible. Because this system is not linear in $\sin(\theta_{i,j})$, it is more difficult to find the values for which this is possible than if the $\sin(\theta_{3,2} + \theta_{2,1})$ term was not present allowing the system to be solved for each $\sin(\theta_{i,j})$. This will be possible for the chain system. However, it can be numerically determined for what values of $\Delta_{2,1}/D$ and $\Delta_{3,2}/D$ there are values of $\theta_{i,j}$ that solve the equations for $\dot{\theta}_{2,1} = \dot{\theta}_{3,2} = 0$. Then within this region, the smallest square can be found.

For this system, the following Arnold tongue is obtained:

$$\left|\frac{\Delta_{i,j}}{D}\right| \leq 0.88, \tag{2.32}$$

for the i, j specified in Equations (2.30) and (2.31). this bound is smaller than in the two oscillator system.

2.5.2. Synchronisation of three chain coupled van der Pol oscillators

Three van der Pol oscillators coupled in a chain have the following equations for their phases:

$$\dot{\phi}_1 = -\Omega_1 + \frac{D}{2}\left(\sin(\phi_2 - \phi_1)\right), \tag{2.33}$$

$$\dot{\phi}_2 = -\Omega_2 + \frac{D}{2}\left(\sin(\phi_1 - \phi_2) + \sin(\phi_3 - \phi_2)\right), \tag{2.34}$$

$$\dot{\phi}_3 = -\Omega_3 + \frac{D}{2}\left(\sin(\phi_2 - \phi_3)\right). \tag{2.35}$$

The phase differences can then be written as

$$\dot{\theta}_{2,1} = -\Delta_{2,1} + \frac{D}{2}\left(-2\sin(\theta_{2,1}) + \sin(\theta_{3,2})\right), \tag{2.36}$$

$$\dot{\theta}_{3,2} = -\Delta_{3,2} + \frac{D}{2}\left(\sin(\theta_{2,1}) - 2\sin(\theta_{3,2})\right). \tag{2.37}$$

$$\tag{2.38}$$

Setting the terms on the l.h.s to 0, allows this system to be solved analytically for $\sin(\theta_{i,j})$:

$$\sin(\theta_{2,1}) = \frac{2}{3D}\left(-2\Delta_{2,1} - \Delta_{3,2}\right), \tag{2.39}$$

$$\sin(\theta_{3,2}) = \frac{2}{3D}\left(-\Delta_{2,1} - 2\Delta_{3,2}\right). \tag{2.40}$$

Introducing the bound $|\sin(\theta_{i,j}| \leq 1$ leads to the following Arnold tongue:

$$\left|\frac{\Delta_{i,j}}{D}\right| \leq 0.5. \tag{2.41}$$

2.6. Synchronisation of four van der Pol oscillators

There are six ways to couple four oscillators, shown in Figure 2.5. These are the six connected graphs with four vertices. They have been given names so that they can be easily referenced to during the paper, however these names are not general use.

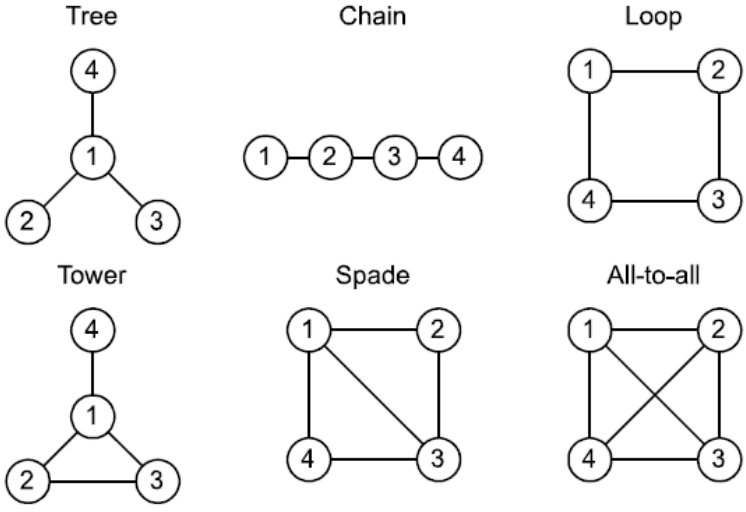

Figure 2.5: Six ways to connect four oscillators. The names have been given solely for the purpose of referencing to them throughout this paper. Each oscillator has been numbered to make clear what is referred to by oscillator i throughout the paper.

Each of these systems will show different synchronisation behaviour. Both the tree and the chain can be seen as extensions of the three chain coupled oscillator system. The loop and all-to-all systems can both be seen as extensions of the three all-to-all coupled oscillator system. The "tower" and the "spade" systems are more unique. The systems will be treated in order of ascending number of couplings.

2.6.1. Synchronisation in the tree system

The equations for the phase of the oscillators in a tree system are as follows:

$$\dot{\phi_1} = -\Omega_1 + \frac{D}{2}\left(\sin(\phi_4 - \phi_1) + \sin(\phi_3 - \phi_1) + \sin(\phi_2 - \phi_1)\right), \tag{2.42}$$

$$\dot{\phi_2} = -\Omega_2 + \frac{D}{2}\left(\sin(\phi_1 - \phi_2)\right), \tag{2.43}$$

$$\dot{\phi_3} = -\Omega_3 + \frac{D}{2}\left(\sin(\phi_1 - \phi_3)\right), \tag{2.44}$$

$$\dot{\phi_4} = -\Omega_4 + \frac{D}{2}\left(\sin(\phi_1 - \phi_4)\right). \tag{2.45}$$

This leads to the following equations for the phase differences (all with respect to oscillator 1):

$$\dot{\theta}_{1,2} = -\Delta_{1,2} + \frac{D}{2}\left(-2\sin(\theta_{1,2}) - \sin(\theta_{1,3}) - \sin(\theta_{1,4})\right), \tag{2.46}$$

$$\dot{\theta}_{1,3} = -\Delta_{1,3} + \frac{D}{2}\left(-\sin(\theta_{1,2}) - 2\sin(\theta_{1,3}) - \sin(\theta_{1,4})\right), \tag{2.47}$$

$$\dot{\theta}_{1,4} = -\Delta_{1,4} + \frac{D}{2}\left(-\sin(\theta_{1,2}) - \sin(\theta_{1,3}) - 2\sin(\theta_{1,4})\right). \tag{2.48}$$

Setting all the terms on the left hand side to zero allows the system to be solved for each $\sin(\theta_{i,j})$:

$$\sin(\theta_{1,2}) = \frac{1}{2D}(-3\Delta_{1,2} + \Delta_{1,3} + \Delta_{1,4}), \tag{2.49}$$

$$\sin(\theta_{1,3}) = \frac{1}{2D}(\Delta_{1,2} - 3\Delta_{1,3} + \Delta_{1,4}), \tag{2.50}$$

$$\sin(\theta_{1,4}) = \frac{1}{2D}(\Delta_{1,2} + \Delta_{1,3} - 3\Delta_{1,4}). \tag{2.51}$$

Each equation has the bound $|\sin(\theta_{1,j})| \leq 1$ meaning that the Arnold tongue is given by

$$\left|\frac{\Delta_{1,j}}{D}\right| \leq 0.4. \tag{2.52}$$

The Arnold tongue has shrunk slightly compared to the three oscillators coupled in a chain (which is essentially a tree).

2.6.2. Synchronisation in the chain system

The equations for the phase of the oscillators in a chain system are as follows:

$$\dot{\phi_1} = -\Omega_1 + \frac{D}{2}\left(\sin(\phi_2 - \phi_1)\right), \tag{2.53}$$

$$\dot{\phi_2} = -\Omega_2 + \frac{D}{2}\left(\sin(\phi_3 - \phi_2) + \sin(\phi_1 - \phi_2)\right), \tag{2.54}$$

$$\dot{\phi_3} = -\Omega_3 + \frac{D}{2}\left(\sin(\phi_4 - \phi_3) + \sin(\phi_2 - \phi_3)\right), \tag{2.55}$$

$$\dot{\phi_4} = -\Omega_4 + \frac{D}{2}\left(\sin(\phi_3 - \phi_4)\right), \tag{2.56}$$

giving the following equations for the phase differences:

$$\dot{\theta}_{2,1} = -\Delta_{2,1} + \frac{D}{2}\left(-2\sin(\theta_{1,2}) + \sin(\theta_{3,2})\right), \tag{2.57}$$

$$\dot{\theta}_{3,2} = -\Delta_{3,2} + \frac{D}{2}\left(\sin(\theta_{2,1}) - 2\sin(\theta_{3,2}) + \sin(\theta_{4,3})\right), \tag{2.58}$$

$$\dot{\theta}_{4,3} = -\Delta_{4,3} + \frac{D}{2}\left(\sin(\theta_{3,2}) - 2\sin(\theta_{3,4})\right). \tag{2.59}$$

This system is also solvable for the $\sin(\theta_{i,j})$'s when each term on the left is set to 0, and subsequently gives the following Arnold tongue:

$$\left|\frac{\Delta_{i,j}}{D}\right| \leq 0.25, \tag{2.60}$$

for the i, j mentioned in Equations (2.57)-(2.59).

Notice how when an extra oscillator was added to the two "chain" coupled oscillators, the bound halved, and now when another oscillator is added in the chain the bound has halved again. This pattern may be interesting to investigate for N oscillators coupled in a chain.

2.6.3. Synchronisation in the loop system

The phase equations do not change much when adding new coupling. Introducing the coupling between oscillator i and oscillator j adds the term $\frac{D}{2}\sin(\phi_j - \phi_i)$ to the equation for $\dot{\phi}_i$ and vice versa for $\dot{\phi}_j$. For this reason, the phase equations will not be written out explicitly for the following systems, instead proceeding straight to the phase difference equations. For the loop system, they are as follows:

$$\dot{\theta}_{2,1} = -\Delta_{2,1} + \frac{D}{2}\left(-2\sin(\theta_{2,1}) + \sin(\theta_{3,2}) - \sin(\theta_{4,3} + \theta_{3,2} + \theta_{2,1})\right), \tag{2.61}$$

$$\dot{\theta}_{3,2} = -\Delta_{3,2} + \frac{D}{2}\left(\sin(\theta_{2,1}) - 2\sin(\theta_{3,2}) + \sin(\theta_{4,3})\right), \tag{2.62}$$

$$\dot{\theta}_{4,3} = -\Delta_{4,3} + \frac{D}{2}\left(\sin(\theta_{3,2}) - 2\sin(\theta_{4,3}) - \sin(\theta_{4,3} + \theta_{3,2} + \theta_{2,1})\right). \tag{2.63}$$

$$\tag{2.64}$$

The Arnold tongue is difficult to find analytically, but just as for the three all-to-all coupled oscillators, it can be found numerically. This is also the case for the rest of the 4-oscillator systems. The Arnold tongue found is

$$\left|\frac{\Delta_{i,j}}{D}\right| \leq 0.45(\pm 0.01), \tag{2.65}$$

where the uncertainty has been included in the brackets to emphasise that this value was found numerically and may deviate slightly from the true upper bound.

2.6.4. Synchronisation in the tower system

The phase differences in the tower system are as follows (for this system, each phase difference is formulated with respect to oscillator 1):

$$\dot{\theta}_{1,2} = -\Delta_{1,2} + \frac{D}{2}\left(-2\sin(\theta_{1,2}) - \sin(\theta_{1,3}) - \sin(\theta_{1,4}) + \sin(\theta_{3,1} - \theta_{2,1})\right), \tag{2.66}$$

$$\dot{\theta}_{1,3} = -\Delta_{1,3} + \frac{D}{2}\left(-\sin(\theta_{1,2}) - 2\sin(\theta_{1,3}) - \sin(\theta_{1,4}) - \sin(\theta_{3,1} - \theta_{2,1})\right), \tag{2.67}$$

$$\dot{\theta}_{1,4} = -\Delta_{1,4} + \frac{D}{2}\left(-\sin(\theta_{1,2}) - \sin(\theta_{1,3}) - 2\sin(\theta_{1,4})\right). \tag{2.68}$$

Then the numerically evaluated bound is

$$\left|\frac{\Delta_{1,j}}{D}\right| \leq 0.40(\pm 0.01). \tag{2.69}$$

Interestingly, this bound is very similar to that for the tree system, indicating that adding the extra coupling does not increase the domain of values for which synchronisation is possible. It is emphasised that the phase and frequency differences are with respect to oscillator 1, although a connection between oscillator 2 and 3 is present. This means that the bound is only for frequency differences w.r.t oscillator 1, so actually a frequency difference of $0.8D$ is possible between oscillator and 2 and 3 while still allowing for synchronisation.

2.6.5. Synchronisation in the spade system

The spade system is simply the all-to-all system with one coupling missing. The phase differences in the spade system are given by the following equations:

$$\dot{\theta}_{2,1} = -\Delta_{2,1} + \frac{D}{2}\left(-2\sin(\theta_{2,1}) + \sin(\theta_{3,2}) - \sin(\theta_{3,2}+\theta_{2,1}) - \sin(\theta_{4,3}+\theta_{3,2}+\theta_{2,1})\right), \tag{2.70}$$

$$\dot{\theta}_{3,2} = -\Delta_{3,2} + \frac{D}{2}\left(\sin(\theta_{2,1}) - 2\sin(\theta_{3,2}) + \sin(\theta_{4,3}) - \sin(\theta_{3,2}+\theta_{2,1})\right), \tag{2.71}$$

$$\dot{\theta}_{4,3} = -\Delta_{4,3} + \frac{D}{2}\left(\sin(\theta_{3,2}) - 2\sin(\theta_{4,3}) + \sin(\theta_{3,2}+\theta_{2,1}) - \sin(\theta_{4,3}+\theta_{3,2}+\theta_{2,1})\right). \tag{2.72}$$

From these equations, the Arnold tongue can numerically be evaluated to be

$$\left|\frac{\Delta_{i,j}}{D}\right| \leq 0.60(\pm 0.01). \tag{2.73}$$

2.6.6. Synchronisation in the all-to-all coupled system

The final system to be analysed is one in which each oscillator is coupled to each other oscillator. The phase differences are

$$\dot{\theta}_{2,1} = -\Delta_{2,1} + \frac{D}{2}\left(-2\sin(\theta_{2,1}) + \sin(\theta_{3,2}) - \sin(\theta_{3,2}+\theta_{2,1}) + \sin(\theta_{4,3}+\theta_{3,2}) - \sin(\theta_{4,3}+\theta_{3,2}+\theta_{2,1})\right), \tag{2.74}$$

$$\dot{\theta}_{3,2} = -\Delta_{3,2} + \frac{D}{2}\left(\sin(\theta_{2,1}) - 2\sin(\theta_{3,2}) + \sin(\theta_{4,3}) - \sin(\theta_{3,2}+\theta_{2,1}) - \sin(\theta_{4,3}+\theta_{3,2})\right), \tag{2.75}$$

$$\dot{\theta}_{4,3} = -\Delta_{4,3} + \frac{D}{2}\left(\sin(\theta_{3,2}) - 2\sin(\theta_{4,3}) + \sin(\theta_{3,2}+\theta_{2,1}) - \sin(\theta_{4,3}+\theta_{3,2}) - \sin(\theta_{4,3}+\theta_{3,2}+\theta_{2,1})\right). \tag{2.76}$$

The bound found for the all-to-all coupled system is

$$\left|\frac{\Delta_{i,j}}{D}\right| \leq 0.84(\pm 0.01). \tag{2.77}$$

This is only slightly less than the equivalent case for three oscillators.

2.7. Comparing Arnold tongues

The Arnold tongues found for every system of coupled oscillators discussed are displayed in Table 2.1. For the two and three oscillator system the result has also been listed for the other categories presented in Section 2.6, despite these categories being different from the original names. This is because they are technically the same type of system. (For example, the three chain coupled oscillators is also classified as a tree, as well as the two coupled oscillators.)

Table 2.1: Table showing the Arnold tongues found in the previous sections for different coupling systems. The value displayed is the upper bound K in $\left|\frac{\Delta_{i,j}}{D}\right| \leq K$ which determines when synchronisation is possible. For the tree and tower system, the bound refers to $\Delta_{1,j}/D$.

	Tree	Chain	Loop	Tower	Spade	All-to-all
Two	1	1	1	-	-	1
Three	0.5	0.5	0.88	-	-	0.88
Four	0.4	0.25	0.45	0.40	0.60	0.84

There is a trend that for a specific number of oscillators, more connections between oscillators leads to a larger Arnold tongue. This is expected as more connections mean the oscillators have a greater effect on each other, increasing coupling.

There is also a trend that systems with more oscillators are harder to synchronise. It would be interesting to see how the synchronisation regimes change when the tree, chain, loop and all-to-all systems are investigated with N oscillators, although this is outside the scope of this thesis.

For systems with the same number of connections, there is now a difference based on the geometry. The tree system is easier to synchronise than the chain system, which can be reasoned to be because for synchronisation to occur, all of the oscillators have to be synchronised. Because in the chain system the first oscillator is three connections away from the fourth oscillator, synchronisation is more difficult than in the tree system where the maximum distance between two oscillators is two. The increased difficulty to synchronise for the tower system compared to the loop system can be justified by the difference in their geometries. In the tower system the fourth oscillator is only coupled to one other oscillator while in the loop system each oscillator has a coupling on either side.

Figure 2.6 displays the Arnold tongues for each of the four oscillators systems. As long as values are chosen above the lines, synchronisation will be possible. Note that on the y-axis is $V = 2D$ to make comparison easier for results on quantum synchronisation later in the paper.

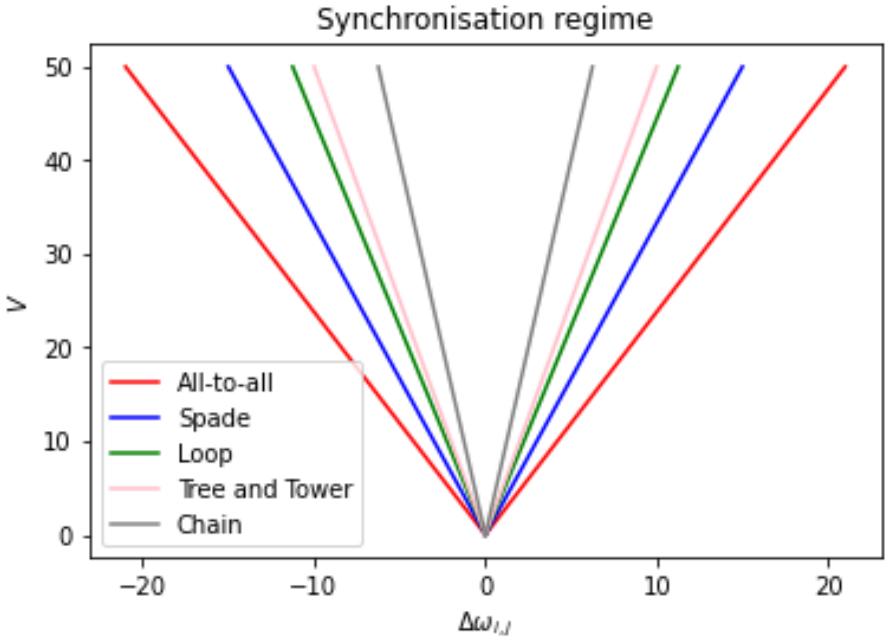

Figure 2.6: Synchronisation regimes for each of the four oscillator systems discussed. As long as value is chosen above the respective line, synchronisation will be possible for that system. $V = 2D$.

In this chapter two different classical models where synchronisation was possible have been discussed: First the simple discrete model and second systems involving coupled van der Pol oscillators. The conditions required for synchronisation to be possible in these systems were subsequently established. In Chapter 4, these models are extended with quantum mechanical effects. However before these models can be investigated, Chapter 3 explains some key notions in quantum mechanics, including the origin of the quantum van der Pol oscillator.

3

Quantum Theory

3.1. Qubit

A qubit refers to any quantum system that can take on two levels. The "quantum" aspect of the qubit comes from the fact that instead of only being able to be in the state $|0\rangle$ or $|1\rangle$, it can also be in a superposition of the two states $|\psi\rangle = c_1|0\rangle + c_2|1\rangle$ such that the total probability of being in a state is 1: $\langle\psi|\psi\rangle = |c_1|^2 + |c_2|^2 = 1$.

A geometrical representation for the state of a qubit can be obtained by projecting the qubit onto a *Bloch sphere*, shown in Figure 3.1.

The state can be written in terms of angles on such a sphere. This is done by first shifting the state of the qubit such that c_1 is real, and then defining

$$|\psi\rangle = \cos\left(\frac{\theta}{2}\right)|0\rangle + \left(\cos(\phi) + i\sin(\phi)\right)\sin\left(\frac{\theta}{2}\right)|1\rangle, \tag{3.1}$$

with $0 \leq \theta \leq \pi$ and $0 \leq \phi \leq 2\pi$.

The parameters θ and ϕ determine the position on the sphere via the vector $\vec{a} = (\sin\theta\cos\phi, \sin\theta\sin\phi, \cos\theta)$.

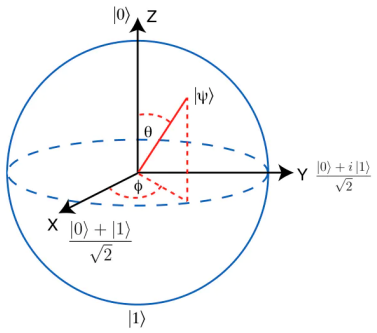

Figure 3.1: Bloch sphere representation of a qubit. [8]

3.2. Density matrix

The concept of the wave function $|\psi\rangle$ to describe the state of a physical object will be familiar. However often physical objects may not be perfectly controlled. Suppose there is only statistical information about the prepared states; this can be called an ensemble of pure states $|\psi_j\rangle$, each with a probability p_j. To describe such a system, the density operator/matrix [1] is used, defined by

$$\rho = \sum_j p_j |\psi_j\rangle\langle\psi_j|. \tag{3.2}$$

such that the $\sum_j p_j = 1$.

The density operator is a very useful way of describing the state of a system as well as the time-evolution of a system. For a wave function, the evolution can be described by the Schrödinger equation :

$$i\hbar\frac{d}{dt}|\psi\rangle = \hat{H}|\psi\rangle. \tag{3.3}$$

For the density operator, the time evolution is described by the *von Neumann equation*:

$$i\hbar\frac{\partial\rho}{\partial t} = [H, \rho]. \tag{3.4}$$

[1] The terms *operator* and *matrix* are often used interchangeably. Technically, the density matrix is obtained by choosing the basis on which the density operator is applied.

where $[A,B] = AB - BA$ is the commutator.

In the case that the Hamiltonian is time-independent, this equation can be solved to arrive at

$$\rho(t) = e^{-iHt/\hbar}\rho(0)e^{iHt/\hbar}. \tag{3.5}$$

Another key property of the density operator, is that the expected values of observables can be calculated very easily, using

$$\langle A \rangle = \mathrm{tr}(\rho A). \tag{3.6}$$

An important value for a density matrix is its *purity*. For pure states, the density matrix can be written as $\rho = |\psi\rangle\langle\psi|$, i,e there is only one state present in the statistical ensemble. This also means the density matrix is idempotent:

$$\rho^2 = |\psi\rangle\langle\psi||\psi\rangle\langle\psi| = |\psi\rangle\langle\psi| = \rho, \tag{3.7}$$

where it is used that $\langle\psi|\psi\rangle = 1$. The purity is defined by

$$\text{purity} = \mathrm{Tr}(\rho^2). \tag{3.8}$$

For mixed states this value is lower than 1. The lower the value, the more mixed a state is.

The density matrix of qubits can be expressed on the Bloch sphere. While pure states will always be on the surface of the sphere, mixed states are inside the sphere, where the length of the Bloch vector $\vec{a}$ indicates the purity of the state. Any density matrix for a two level system can be expressed as

$$\rho = \frac{1}{2}(I + \vec{a}\cdot\vec{\sigma}) \tag{3.9}$$

$$= \frac{1}{2}\begin{pmatrix}1 & 0\\ 0 & 1\end{pmatrix} + \frac{a_x}{2}\begin{pmatrix}0 & 1\\ 1 & 0\end{pmatrix} + \frac{a_y}{2}\begin{pmatrix}0 & -i\\ i & 0\end{pmatrix} + \frac{a_z}{2}\begin{pmatrix}1 & 0\\ 0 & -1\end{pmatrix} \tag{3.10}$$

$$= \frac{1}{2}\begin{pmatrix}1+a_z & a_x - i\,a_y\\ a_x + i\,a_y & 1-a_z\end{pmatrix}. \tag{3.11}$$

So for a given density matrix, the respective Bloch vector can be found, which determines a point on the Bloch sphere.

3.3. Quantum harmonic oscillator

One of the first systems studied in an undergraduate course on quantum mechanics is the *quantum harmonic oscillator* [9]. The features of a quantum harmonic oscillator can best be found by quantising the classical harmonic oscillator, whose equation of motion and Hamiltonian are given by:

$$\ddot{x} + \omega^2 x = 0, \tag{3.12}$$

$$H = \frac{p^2}{2m} + \frac{1}{2}m\omega^2 x^2. \tag{3.13}$$

where the first term in the Hamiltonian represent the kinetic energy and the second term represents the potential energy.

Quantising the Hamiltonian involves replacing the position and momentum by the respective *operators* $\hat{x}$ and $\hat{p} = -i\hbar\frac{d}{dx}$.

$$\hat{H} = \frac{\hat{p}^2}{2m} + \frac{1}{2}m\omega^2\hat{x}^2. \tag{3.14}$$

To rewrite this, two new operators are introduced namely the *annihilation*, $\hat{a}$ and *creation*, $\hat{a}^\dagger$ operators given by

$$\hat{a} \equiv \frac{1}{\sqrt{2\hbar m\omega}}(i\hat{p} + m\omega\hat{x}), \tag{3.15}$$

$$\hat{a}^\dagger \equiv \frac{1}{\sqrt{2\hbar m\omega}}(-i\hat{p} + m\omega\hat{x}), \tag{3.16}$$

and the inverse of these relations:

$$\hat{x} = \sqrt{\frac{\hbar}{2m\omega}}(\hat{a} + \hat{a}^\dagger), \tag{3.17}$$

$$\hat{p} = -i\sqrt{\frac{\hbar m\omega}{2}}(\hat{a} - \hat{a}^\dagger), \tag{3.18}$$

This allows the Hamiltonian to be rewritten as

$$\hat{H} = \hbar\omega(\hat{a}^\dagger\hat{a} + \frac{1}{2}). \tag{3.19}$$

The reason why these are called annihilation(creation) operators is because if $\hat{a}(\hat{a}^\dagger)$ is applied to a specific eigenstate, it results in an eigenstate exactly one energy level below(above) the original eigenstate[9].

An important aspect of these operators is that their commutation relation is given by:

$$[\hat{a}, \hat{a}^\dagger] = \hat{a}\hat{a}^\dagger - \hat{a}^\dagger\hat{a} = 1. \tag{3.20}$$

Using Equation (3.19) in combination with the Schrödinger equation, the time evolution of a quantum harmonic oscillator can be determined. However when damping is present, this becomes more difficult. Equations (3.12) and (3.13) lead to the following system of equations for x and p:

$$\dot{x} = \frac{p}{m}, \quad \dot{p} = -m\omega^2 x. \tag{3.21}$$

Quantising this system is perfectly feasible as there exists a Hamiltonian, and importantly the commutation relation between $\hat{x}$ and $\hat{p}$ leads to

$$[\hat{x}, \hat{p}] = i\hbar. \tag{3.22}$$

To illustrate the problem with introducing damping in quantum systems, consider the following classical equation for a damped harmonic oscillator [10]:

$$\ddot{x} + \gamma\dot{x} + \omega^2 x = 0. \tag{3.23}$$

with γ the damping coefficient.

This would lead to the following system of differential equations for x and p:

$$\dot{x} = \frac{p}{m}, \quad \dot{p} = -\gamma p - m\omega^2 x. \tag{3.24}$$

In attempting to generate an equivalent system in quantum mechanics there are some issues. The first issue faced is that this system does not have a respective Hamiltonian, meaning that there is no way for the Schrödinger equation to describe the evolution of the system as it requires a Hamiltonian. The second issue concerns the time evolution of the commutation relation between $\hat{x}$ and $\hat{p}$. If x and p are converted into operators $\hat{x}$ and $\hat{p}$ then

$$\begin{aligned}\frac{d}{dt}[\hat{x}, \hat{p}] &= \dot{\hat{x}}\hat{p} + \hat{x}\dot{\hat{p}} - \dot{\hat{p}}\hat{x} - \hat{p}\dot{\hat{x}} \\ &= -\frac{\hat{p}^2}{m} - \gamma\hat{x}\hat{p} - m\omega^2\hat{x}^2 - (-\gamma\hat{p}\hat{x} - m\omega^2 x^2 - \frac{\hat{p}^2}{m}) \\ &= -\gamma\hat{x}\hat{p} + \gamma\hat{p}\hat{x} = -\gamma[\hat{x}, \hat{p}].\end{aligned} \tag{3.25}$$

This equation has the following solution:

$$[\hat{x}, \hat{p}] = e^{-\gamma t}[\hat{x}(0), \hat{p}(0)] = e^{-\gamma t} i\hbar. \tag{3.26}$$

This means that with time, this commutator actually decays. However if we apply this to the Heisenberg uncertainty relation, then

$$\sigma_x \sigma_p \geq \frac{1}{2}\hbar e^{-\gamma t}, \tag{3.27}$$

meaning that the uncertainties also decay to 0.

From these results the conclusion can be drawn that incorporating damping into a quantum mechanical system is not as straightforward as in a classical system. Although the current results have been derived from a simple damped harmonic oscillator, the van der Pol oscillator (Equation (2.8)) similarly does not have a corresponding Hamiltonian [2] and as a result, quantising it meets the same difficulties.

Other approaches taking into account dissipation in quantum oscillators have been proposed, such that their synchronisation behaviour can be investigated. The widely accepted approach involves coupling between the system and a reservoir. In this approach damping takes place by exchanging photons with the reservoir, which is subsequently traced out such that only the original system remains. A derivation for the time evolution of a damped system will be performed later in the paper, however first some key concepts will be explained.

3.4. Interaction picture

A very important tool that will be used in the derivation is performing calculations in the interaction picture. Most often, calculations in quantum mechanics are performed in the Schrödinger picture, where the state changes with time while the observables are time-independent. Another commonly used picture is the Heisenberg picture, where the state is kept constant, but the observables change in time. The *interaction picture* lies in between these two pictures.

Suppose a state is in the Schrödinger picture, with Hamiltonian H_S. The Hamiltonian can be split into two parts $H_{0,S}$ and $H_{1,S}$. Usually, these two Hamiltonians are chosen such that $H_{0,S}$ is well understood, while $H_{1,S}$ is a more difficult to understand perturbation. Supposing that $H_{0,S}$ is time-independent, the operators and states can then be rewritten in the interaction picture:

$$\rho_I(t) = e^{iH_{0,S}t/\hbar}\rho_S(t)e^{-iH_{0,S}t/\hbar}, \tag{3.28}$$

$$A_I(t) = e^{iH_{0,S}t/\hbar}A_S(t)e^{-iH_{0,S}t/\hbar}. \tag{3.29}$$

This is a transformation which will be very useful in the derivation. First, there is one more feature in this picture to discuss.

3.5. Rotating wave approximation

When discussing the coupling between two classical oscillators, one of the ways in which this coupling could be implemented was to include an $x_1 \cdot x_2$ term in the Hamiltonian. This would subsequently lead to an x_1 term in the equation of motion for x_2 and vice versa.

If two quantum harmonic oscillators were coupled this way, the Hamiltonian would be written as

$$\hat{H} = \hbar\omega_1 \hat{a}_1^\dagger \hat{a}_1 + \hbar\omega_2 \hat{a}_2^\dagger \hat{a}_2 + \hat{x_1}\hat{x_2}. \tag{3.30}$$

where the $\frac{1}{2}\hbar\omega$ term present in Equation (3.19) has been neglected as it does not contribute to the dynamics (this zero point energy energy can be ignored by performing a shift in the energy such that the constant term is not present).

Rewriting the coupling term in terms of annihilation/creation operators using Equation (3.17) leads to

[2] A Hamiltonian for the classical van der Pol oscillator can be generated by using an auxiliary coupled to the original system, however this still cannot be used to quantise the van der Pol oscillator [11].

$$\begin{aligned}\hat{x}_1\hat{x}_2 &= \frac{\hbar}{2\sqrt{m_1 m_2\omega_1\omega_2}}(\hat{a}_1 + \hat{a}^\dagger{}_1)(\hat{a}_2 + \hat{a}^\dagger{}_2),\\ &= \frac{\hbar}{2\sqrt{m_1 m_2\omega_1\omega_2}}(\hat{a}_1\hat{a}_2 + \hat{a}_1^\dagger\hat{a}_2 + \hat{a}_1\hat{a}_2^\dagger + \hat{a}_1^\dagger\hat{a}_2^\dagger).\end{aligned} \tag{3.31}$$

The rotating wave approximation involves removing the terms $\hat{a}_1^\dagger\hat{a}_2^\dagger$ and $\hat{a}_1\hat{a}_2$. This is due to these two terms being fast oscillating so they can be neglected in the approximation. The full approximation is shown in Appendix A.2.

The $\hat{x}_1\hat{x}_2$ in Equation (3.30) is replaced by

$$C\cdot(\hat{a}_1^\dagger\hat{a}_2 + \hat{a}_1\hat{a}_2^\dagger). \tag{3.32}$$

with C a constant.

These concepts are used to derive an equation to describe an evolution of a quantum damped (or van der Pol) harmonic oscillator. Before the derivation is performed, the goal will be formulated.

3.6. Master equations

The goal is to derive a master equation for the evolution of a system (in this case either a damped quantum harmonic oscillator or a quantum van der Pol oscillator). This master equation is known as a Lindblad equation and will be of the following form [12] :

$$\dot{\rho} = -i[H,\rho] + \sum_k A_k\rho A_k^\dagger - \frac{1}{2}(A_k^\dagger A_k\rho + \rho A_k^\dagger A_k), \tag{3.33}$$

where H represent the Hamiltonian of the system, and the A_k's represent different operators that describe the damping in the system.

This equation describes how the state ρ will evolve over time, in a similar way to how the Schrödinger equation describes how a state evolves over time. The master equation can be used in systems that are complex, at the cost of some approximations being made to the system.

The terms in the summation are usually replaced by the Lindlbad superoperator $\mathcal{D}[A_k](\rho) = A_k\rho A_k^\dagger - \frac{1}{2}(A_k^\dagger A_k\rho + \rho A_k^\dagger A_k)$ which makes the damping terms present in a system more explicit. For the damped harmonic oscillator, the master equation that will be derived is

$$\dot{\rho} = -\frac{i}{\hbar}[H,\rho] + \gamma_\downarrow\mathcal{D}[\hat{a}](\rho) + \gamma_\uparrow\mathcal{D}[\hat{a}^\dagger](\rho), \tag{3.34}$$

with $H = \hbar\omega\hat{a}^\dagger\hat{a}$.

Here the usual Hamiltonian is present for a quantum harmonic oscillator, with two additional damping terms. The first term describes damping via the annihilation operator $\hat{a}$, while the second operator describes negative damping via the creation operator $\hat{a}^\dagger$.

The quantum van der Pol oscillator takes a slightly different form:

$$\dot{\rho} = -\frac{i}{\hbar}[H,\rho] + \gamma_\downarrow\mathcal{D}[\hat{a}^2](\rho) + \gamma_\uparrow\mathcal{D}[\hat{a}^\dagger](\rho). \tag{3.35}$$

Due to the $\hat{a}^2$ term, there is non-linear damping present in the system, mirroring the non-linear damping in the classical van der Pol oscillator. In the quantum limit $\gamma_\uparrow \ll \gamma_\downarrow$, only the lowest states are occupied and the higher states can be ignored. This is due to the damping term $\mathcal{D}[\hat{a}^2](\rho)$ term dominating, causing higher states to be annihilated down to lower states. In the classical limit $\gamma_\uparrow \gg \gamma_\downarrow$, the negative damping term $\mathcal{D}[\hat{a}^\dagger](\rho)$ causes the higher states to be occupied, while lower states are empty. In this limit, the discrete nature of the energy levels becomes negligible so the oscillator begins to mimic a classical oscillator which has a continuous energy spectrum. This means the operator $\langle\hat{a}\rangle$ can be replaced by a coherent state allowing an analogy to be made between the classical van der Pol oscillator and the quantum van der Pol oscillator via the amplitude equation. This is done by looking at the time evolution of $\langle\hat{a}\rangle$, the expected value of the annihilation operator. This will take the place of A in the amplitude equation. First,

$$\frac{d\langle\hat{a}\rangle}{dt} = \frac{d\mathrm{Tr}(\rho\hat{a})}{dt} = \frac{d\sum_i\sum_j\rho_{i,j}\hat{a}_{j,i}}{dt} = \sum_i\sum_j\frac{d\rho_{i,j}}{dt}\hat{a}_{j,i} + \rho_{i,j}\frac{d\hat{a}_{j,i}}{dt}. \tag{3.36}$$

The annihilation operator itself is constant in time, so only the first term needs to be considered, which can be rewritten as $\mathrm{Tr}(\dot{\rho}\hat{a})$. Now the master equation, Equation (3.35), can be inserted. Due to the linearity of the trace, each term in $\dot{\rho}$ can be evaluated individually. Beginning with the Hamiltonian term:

$$\begin{aligned}\mathrm{Tr}(-\frac{i}{\hbar}[H,\rho]\hat{a}) &= \mathrm{Tr}(-i\omega(\hat{a}^\dagger\hat{a}\rho\hat{a}-\rho\hat{a}^\dagger\hat{a}\hat{a}) = -i\omega\mathrm{Tr}(\hat{a}\hat{a}^\dagger\hat{a}\rho-\hat{a}^\dagger\hat{a}\hat{a}\rho)\\ &= -i\omega\mathrm{Tr}([\hat{a},\hat{a}^\dagger]\hat{a}\rho) = -i\omega Tr(\hat{a}\rho) = -i\omega\langle\hat{a}\rangle,\end{aligned} \tag{3.37}$$

where the commutation relation, Equation (3.20), has been used, along with the cylic invariance property of the trace: $\mathrm{Tr}(ABC) = \mathrm{Tr}(BCA) = \mathrm{Tr}(CAB)$.

Now evaluating the second term:

$$\begin{aligned}\mathrm{Tr}\left(\gamma_\downarrow\mathcal{D}[\hat{a}^2](\rho)\hat{a}\right) &= \mathrm{Tr}\left(\gamma_\downarrow[\hat{a}^2\rho\hat{a}^{2\dagger}-\frac{1}{2}(\hat{a}^{2\dagger}\hat{a}^2\rho+\rho\hat{a}^{2\dagger}\hat{a}^2)]\hat{a}\right) = \gamma_\downarrow\mathrm{Tr}\left(\hat{a}^{2\dagger}\hat{a}^3\rho-\frac{1}{2}(\hat{a}\hat{a}^{2\dagger}\hat{a}^2\rho+\hat{a}^{2\dagger}\hat{a}^3\rho)\right)\\ &= \gamma_\downarrow\mathrm{Tr}\left(\frac{1}{2}(-\hat{a}\hat{a}^{2\dagger}\hat{a}^2\rho+\hat{a}^{2\dagger}\hat{a}^3\rho)\right) = \frac{1}{2}\gamma_\downarrow\mathrm{Tr}\left(-\hat{a}^\dagger\hat{a}\hat{a}^\dagger\hat{a}^2\rho-\hat{a}^\dagger\hat{a}^2\rho+\hat{a}^{2\dagger}\hat{a}^3\rho\right)\\ &= \frac{1}{2}\gamma_\downarrow\mathrm{Tr}\left(-2\hat{a}^\dagger\hat{a}^2\rho\right) = -\gamma_\downarrow\langle\hat{a}^\dagger\hat{a}^2\rangle.\end{aligned} \tag{3.38}$$

Then finally the third term:

$$\begin{aligned}\mathrm{Tr}\left(\gamma_\uparrow\mathcal{D}[\hat{a}^\dagger](\rho)\hat{a}\right) &= \gamma_\uparrow\mathrm{Tr}\left([\hat{a}^\dagger\rho\hat{a}-\frac{1}{2}(\hat{a}\hat{a}^\dagger\rho+\rho\hat{a}\hat{a}^\dagger]\hat{a}\right) = \gamma_\uparrow\mathrm{Tr}\left(\hat{a}^2\hat{a}^\dagger\rho-\frac{1}{2}(\hat{a}^2\hat{a}^\dagger+\hat{a}\hat{a}^\dagger\hat{a}\rho)\right)\\ &= \frac{1}{2}\gamma_\uparrow\mathrm{Tr}\left(\hat{a}[\hat{a},\hat{a}^\dagger]\rho\right) = \frac{1}{2}\gamma_\uparrow\langle\hat{a}\rangle.\end{aligned} \tag{3.39}$$

Combining these results leads to the following equation for $\langle\hat{a}\rangle$:

$$\frac{d\langle\hat{a}\rangle}{dt} = -i\omega\langle\hat{a}\rangle-\gamma_\downarrow\langle\hat{a}^\dagger\hat{a}^2\rangle+\frac{1}{2}\gamma_\uparrow\langle\hat{a}\rangle. \tag{3.40}$$

In the classical limit, $\hat{a}$ can be replaced by a coherent state A giving a formula very similar to the amplitude equation:

$$\frac{dA}{dt} = -i\omega A-\gamma_\downarrow|A|^2A+\frac{1}{2}\gamma_\uparrow A. \tag{3.41}$$

The only difference between Equation (3.41) and Equation (2.14) is the presence of the term proportional to ω. This can be removed if the master equation, Equation (3.35), is transformed to take place in a rotating frame.

In the following section the two master equations previously mentioned will be derived. Note that from now on the annihilation operator $\hat{a}$ will be written simply as a however it is important to remember that this is still an operator and not a variable.

3.7. Derivation of the master equation

The master equations in Equations (3.34) and (3.35) can be derived by considering the interaction between a system containing the oscillators of interest, and a reservoir around it. The damping in these oscillators will then occur via energy loss and gain to this reservoir, which is assumed to be large enough that gaining this energy has no effect. This means the temperature of the reservoir can be kept constant. By subsequently tracing out this reservoir, the master equation for the system can be obtained.

This section starts by considering the interaction between a general system and reservoir. Subsequently, the Hamiltonians will be specified such that the master equation for the damped quantum harmonic oscillator can be derived, and then using this result, a master equation very close to that for the van der Pol oscillator will be derived. The results presented here mostly follow the derivation in [10],[13].

3.7.1. Born-Markov equation

First of all, the Hamiltonian of the system and reservoir is split into three parts: the individual Hamiltonians of each along with the interaction between them:

$$H = H_S + H_R + H_{SR}, \tag{3.42}$$

where H_S and H_R represent the Hamiltonians system and reservoir respectively, while H_{SR} describes the coupling between them. For now these Hamiltonians are not specified but later they will be specified to arrive at the desired master equation.

The total state can be described by the density matrix $\rho_T(t)$ and the evolution of this state is described by the von Neumann equation:

$$\dot{\rho}_T = \frac{1}{i\hbar}[H, \rho_T]. \tag{3.43}$$

The state that is of interest is the state of the system only which can be found by tracing out the reservoir and is denoted by ρ:

$$\rho = \mathrm{Tr}_R[\rho_T]. \tag{3.44}$$

Equation (3.43) transformed into the interaction picture in order to separate the expected fast motion generated by H_S and H_R from the slow motion from the interaction H_{SR}. This is done by introducing

$$\tilde{\rho}_T = e^{i/\hbar(H_S+H_R)t}\rho_T e^{-i/\hbar(H_S+H_R)t}, \tag{3.45}$$

$$\tilde{H}_{SR}(t) = e^{i/\hbar(H_S+H_R)t}H_{SR}e^{-i/\hbar(H_S+H_R)t}. \tag{3.46}$$

Equation (3.43) can be rewritten as

$$\dot{\tilde{\rho}}_T = \frac{1}{i\hbar}[\tilde{H}_{SR}(t), \tilde{\rho}_T]. \tag{3.47}$$

By integrating Equation (3.47), an equation for $\tilde{\rho}_T$ is generated which can be substituted back into commutation relation in Equation (3.47):

$$\dot{\tilde{\rho}}_T = \frac{1}{i\hbar}[\tilde{H}_{SR}(t), \rho_T(0)] - \frac{1}{\hbar^2}\int_0^t [\tilde{H}_{SR}(t), [\tilde{H}_{SR}(t'), \tilde{\rho}_T(t')]]\,dt'. \tag{3.48}$$

The equation is currently for the total density state, however only the system is of interest, which can be found by introducing the trace over the reservoir:

$$\dot{\tilde{\rho}} = \mathrm{Tr}_R\left(\frac{1}{i\hbar}[\tilde{H}_{SR}(t), \rho_T(0)] - \frac{1}{\hbar^2}\int_0^t Tr_R[\tilde{H}_{SR}(t), [\tilde{H}_{SR}(t'), \tilde{\rho}_T(t')]]\,dt'\right), \tag{3.49}$$

where $\tilde{\rho}$ is similarly described as in Equation (3.45) but with respect to ρ. This equation is exact, but now some assumptions and approximations are introduced in order to simplify it:

System-reservoir interaction The assumption is made that the interaction between the system and the reservoir only starts at $t = 0$, and that at this point there is no correlation between them. This means that we can separate the total density state $\rho_T(0)$ into two density states $\rho(0)$ and R_0 where R_0 describes the initial state of the reservoir.

Following this assumption, the first term in Equation (3.49) can be set to be 0, an assumption which is exact if the operators coupling R to S have a mean of 0 in the state R_0, which can be guaranteed by adjusting the system Hamiltonian [10].

Born approximation Assuming the coupling is weak, the total state should only deviate slightly from an uncorrelated state so we can extend our first assumption to not just be for $t = 0$:

$$\tilde{\rho}_T(t) \approx \tilde{\rho}(t) \otimes R_0, \tag{3.50}$$

where the assumption is also made that R is a large system and as a result it will largely remain the same despite the coupling to S.

Following these assumptions and approximations, Equation (3.49) can be written as

$$\dot{\tilde{\rho}} = -\frac{1}{\hbar^2}\int_0^t Tr_R[\tilde{H}_{SR}(t),[\tilde{H}_{SR}(t'),\tilde{\rho}(t')\otimes R_0]]\,dt'. \tag{3.51}$$

Markov approximation Equation (3.51) is currently non-Markovian, as the change in state at a specific time does not only depend on its current state, but also on its history, due to integrating over the term $\tilde{\rho}(t')$. The Markov approximation is then to replace this term by $\tilde{\rho}(t)$, so the change in state at a certain time depends only on the current state. This approximation can be justified by reasoning that the reservoir is a very large system, so it will not retain minor changes brought by the coupling to the system for very long. This means that the evolution of S will not be affected very much by its past, as those effects disappear in R, so the evolution of S is only affected by its present state.

With this last approximation the *Born-Markov master equation* is obtained:

$$\dot{\tilde{\rho}} = -\frac{1}{\hbar^2}\int_0^t Tr_R[\tilde{H}_{SR}(t),[\tilde{H}_{SR}(t'),\tilde{\rho}(t)\otimes R_0]]\,dt'. \tag{3.52}$$

3.7.2. Defining the interaction

The model is made slightly more specific by defining H_{SR} as

$$H_{SR} = \hbar\sum_i s_i\Gamma_i, \tag{3.53}$$

where s_i are operators acting only on the system, while Γ_i are operators acting only on the reservoir. Written in the interaction picture, this leads to

$$\tilde{H}_{SR} = \hbar\sum_i \tilde{s}_i(t)\tilde{\Gamma}_i(t), \tag{3.54}$$

$$\tilde{s}_i = e^{i/\hbar H_S t}s_i e^{-i/\hbar H_S t}, \tag{3.55}$$

$$\tilde{\Gamma}_i = e^{i/\hbar H_R t}s_i e^{-i/\hbar H_R t}. \tag{3.56}$$

Substituting this into the Born equation (3.51) (the Markov approximation can be made later) and expanding the commutator gives

$$\begin{aligned}\dot{\tilde{\rho}} = \sum_{i,j}\int_0^t &\{\tilde{s}_i(t)\tilde{s}_j(t')\tilde{\rho}(t') - \tilde{s}_j(t')\tilde{\rho}(t')\tilde{s}_i(t)\}\langle\tilde{\Gamma}_i(t)\tilde{\Gamma}_j(t')\rangle_R \\ &+\{\tilde{\rho}(t')\tilde{s}_j(t')\tilde{s}_i(t) - \tilde{s}_i(t)\tilde{\rho}(t')\tilde{s}_j(t')\}\langle\tilde{\Gamma}_j(t')\tilde{\Gamma}_i(t)\rangle_R\ \ dt',\end{aligned} \tag{3.57}$$

where the environment part has been separated from the system and written as

$$\langle\tilde{\Gamma}_i(t)\tilde{\Gamma}_j(t')\rangle_R = Tr_R[R_0\tilde{\Gamma}_i(t)\tilde{\Gamma}_j(t')], \tag{3.58}$$

$$\langle\tilde{\Gamma}_j(t')\tilde{\Gamma}_i(t)\rangle_R = Tr_R[R_0\tilde{\Gamma}_j(t')\tilde{\Gamma}_i(t)]. \tag{3.59}$$

The Markov approximation relies on the fast decay of these two correlation functions, in which case $\tilde{\rho}(t')$ can be replaced by $\tilde{\rho}(t)$.

Although this model is more specific, it is still very general as the exact setup of the system and the environment has not been specified; only the interaction between them in terms of the operators acting within the system and environment have been specified.

3.7.3. Damped harmonic oscillator

The model will now be formulated specifically for the damped harmonic oscillator. This can subsequently be used to find the master equation for the degenerate parameteric oscillator, and hence the van der Pol oscillator. The model used to derive the equation for the damped harmonic oscillator is given by the following Hamiltonians:

$$H_S \equiv \hbar\omega_0 a^\dagger a, \tag{3.60}$$

$$H_R \equiv \sum_j \hbar\omega_j r_j^\dagger r_j, \tag{3.61}$$

$$H_{SR} \equiv \hbar\left(a\sum_j [\kappa_j^* r^\dagger{}_j] + a^\dagger \sum_j [\kappa_j r_j]\right) \tag{3.62}$$

$$= \hbar(a\Gamma^\dagger + a^\dagger\Gamma). \tag{3.63}$$

The system consists of a harmonic oscillator with annihilation operator a. The reservoir consists of a large amount of harmonic oscillators with annihilation operator r_j, which couples to the system operators a with strength κ_j. In the H_{SR} term the coupling derived in Equation (3.32) under the rotating wave approximation can be observed.

The reservoir is in thermal equilibrium at temperature T. This means that the initial density state can be expressed as [10]:

$$R_0 = \prod_j e^{-\hbar\omega_j r_j^\dagger r_j/k_B T}(1 - e^{-\hbar\omega_j/k_B T}). \tag{3.64}$$

Letting $s_1 = a$, $s_2 = a^\dagger$, $\Gamma_1 = \Gamma^\dagger$ and $\Gamma_2 = \Gamma$, Equation (3.57) can be used. These can then be transformed into the interaction picture using Equations (3.55) and (3.56) leading to:

$$\tilde{s}_1(t) = ae^{-i\omega_0 t}, \tag{3.65}$$

$$\tilde{s}_2(t) = a^\dagger e^{i\omega_0 t}, \tag{3.66}$$

$$\tilde{\Gamma}_1(t) = \sum_j \kappa_j^* r_j^\dagger e^{i\omega_j t}, \tag{3.67}$$

$$\tilde{\Gamma}_2(t) = \sum_j \kappa_j r_j e^{-i\omega_j t}. \tag{3.68}$$

After substituting these into Equation (3.57), the master equation has 16 terms, which can be simplified by considering the reservoir correlations as they are defined in Equations (3.58) and (3.59). These can be calculated to be

$$\langle\tilde{\Gamma}^\dagger(t)\tilde{\Gamma}^\dagger(t')\rangle_R = 0, \tag{3.69}$$

$$\langle\tilde{\Gamma}(t)\tilde{\Gamma}(t')\rangle_R = 0, \tag{3.70}$$

$$\langle\tilde{\Gamma}^\dagger(t)\tilde{\Gamma}(t')\rangle_R = \sum_j |\kappa_j|^2 e^{i\omega_j(t-t')}\bar{n}(\omega_j, T), \tag{3.71}$$

$$\langle\tilde{\Gamma}(t)\tilde{\Gamma}^\dagger(t')\rangle_R = \sum_j |\kappa_j|^2 e^{-i\omega_j(t-t')}[\bar{n}(\omega_j, T) + 1], \tag{3.72}$$

where

$$\bar{n}(\omega_j, T) = Tr_R(R_0 r_j^\dagger r_j) = \frac{e^{-\hbar\omega_j/k_B T}}{1 - e^{-\hbar\omega_j/k_B T}}. \tag{3.73}$$

$\bar{n}(\omega_j, T)$ is the mean photon number for an oscillator in the reservoir with frequency ω_j at temperature T.

Although Equations (3.71) and (3.72) are sums over the reservoir oscillators, these can be changed into an integral by introducing a density of state for the frequencies: $g(\omega)$. This is allowed because the reservoir is assumed to have a very large number of oscillators. This changes the nonzero reservoir correlation functions to

$$\langle\tilde{\Gamma}^\dagger(t)\tilde{\Gamma}(t')\rangle_R = \int_0^\infty e^{i\omega(t-t')} g(\omega)|\kappa(\omega)|^2 \bar{n}(\omega, T)\ \ d\omega, \tag{3.74}$$

$$\langle\tilde{\Gamma}(t)\tilde{\Gamma}^\dagger(t')\rangle_R = \int_0^\infty e^{-i\omega(t-t')} g(\omega)|\kappa(\omega)|^2 (\bar{n}(\omega, T) + 1)\ \ d\omega. \tag{3.75}$$

Using these functions, the validity of the Markov approximation can be investigated based on these correlation functions, the details of which can be found in Chapter 1 of [10]. Including the exponential term in the transformations (3.65) and (3.66) leads to two new parameters:

$$\alpha \equiv \int_0^t \int_0^\infty e^{-i(\omega-\omega_0)(t-t')} g(\omega) \mid \kappa(\omega) \mid^2 \bar{n}(\omega, T) \;\; d\omega dt', \tag{3.76}$$

$$\beta \equiv \int_0^t \int_0^\infty e^{-i(\omega-\omega_0)(t-t')} g(\omega) \mid \kappa(\omega) \mid^2 (\bar{n}(\omega, T)+1) \;\; d\omega dt'. \tag{3.77}$$

With these two parameters, Equation (3.57) can be evaluated into a more familiar version of the master equation:

$$\dot{\tilde{\rho}} = \alpha(a\tilde{\rho}a^\dagger - a^\dagger a\tilde{\rho} + a^\dagger\tilde{\rho}a - \tilde{\rho}a^\dagger a) + 2\beta(a\tilde{\rho}a^\dagger + a^\dagger\tilde{\rho}a - a^\dagger a\tilde{\rho} - \tilde{\rho}aa^\dagger), \tag{3.78}$$

where $\tilde{\rho} = \tilde{\rho}(t)$ due to the Markov approximation.
By evaluating the integrals in Equations (3.76) and (3.77) and defining

$$\gamma \equiv 2\pi g(\omega_0) \mid \kappa(\omega_0) \mid^2, \tag{3.79}$$

$$\bar{n} \equiv \bar{n}(\omega_0, T), \tag{3.80}$$

$$\Delta \equiv P\int_0^\infty \frac{g(\omega) \mid \kappa(\omega) \mid^2}{\omega_0 - \omega}. \tag{3.81}$$

followed by a transformation back into the Schrödinger picture, the master equation for the *damped harmonic oscillator* is produced:

$$\begin{aligned}\dot{\rho} = &-i(\omega_0' + \Delta)[a^\dagger a, \rho] + \frac{\gamma}{2}(2a\rho a^\dagger - a^\dagger a\rho - \rho a^\dagger a) \\ &+ \gamma\bar{n}(a\rho a^\dagger + a^\dagger\rho a - a^\dagger a\rho - \rho aa^\dagger),\end{aligned} \tag{3.82}$$

where $\omega_0' = \omega_0 + \Delta$.
This equation can be rewritten into an explicit form of a Lindblad master equation:

$$\dot{\rho} = -i[\omega_0' a^\dagger, \rho] + \frac{\gamma}{2}\bar{n}(2a^\dagger\rho a - aa^\dagger\rho - \rho aa^\dagger) + \frac{\gamma}{2}(\bar{n}+1)(2a\rho a^\dagger - a^\dagger a\rho - \rho a^\dagger a), \tag{3.83}$$

which is the same as Equation (3.34) with $\gamma_\uparrow = \gamma\bar{n}$ and $\gamma_\downarrow = \gamma(\bar{n}+1)$.

3.7.4. Degenerate parametric oscillator

The degenerate parametric oscillator is similar to the damped harmonic oscillator. "Parametric" refers to the fact that the oscillator is being driven by an external drive, and the term "degenerate" arises from the oscillator of interest (oscillator a) having a natural frequency exactly half that of the drive. It starts with the following Hamiltonians:

$$\begin{aligned}H_S &= \hbar\omega_0 a^\dagger a + \hbar 2\omega_0 b^\dagger b + \frac{i\hbar g}{2}\left(a^{\dagger 2}b - a^2 b^\dagger\right) + \hbar\left(\mathcal{E}_0 e^{-i2\omega_0 t}a^{\dagger 2} + \mathcal{E}_0^* e^{i2\omega_0 t}a^2\right), \\ &\equiv H_a + H_b + H_{ab} + H_{drive}\end{aligned} \tag{3.84}$$

$$H_R = \sum_j \hbar\omega_j r_{aj}^\dagger r_{aj} + \sum_j \omega_j r_{bj}^\dagger r_{bj}, \tag{3.85}$$

$$\begin{aligned}H_{SR} &= H_{SR}^a + H_{SR}^b \\ &= \hbar\left(a\sum_j\left[\kappa_{aj}^* r_{aj}^\dagger\right] + a^\dagger\sum_j\left[\kappa_{aj} r_{aj}\right] + b\sum_j\left[\kappa_{bj}^* r_{bj}^\dagger\right] + b^\dagger\sum_j\left[\kappa_{bj} r_{bj}\right]\right) \\ &\equiv \hbar\left(a\Gamma_a^\dagger + a^\dagger\Gamma_a\right) + \hbar\left(b\Gamma_b^\dagger + b^\dagger\Gamma_b\right)\end{aligned} \tag{3.86}$$

These Hamiltonians have a very similar structure to the ones for the damped harmonic oscillator. There is now a second harmonic oscillator present in the system, which has annihilation operator b and oscillates at a frequency twice that of the original oscillator. The second oscillator will be called the "pump mode" while the original oscillator will be called the "subharmonic mode". The pump mode exchanges photons with its own reservoir with annihilation operator r_{bj}.

The third term in Equation (3.84) describes the interaction between these two modes. Due to the relation between the two modes, there is first an interaction which leads to the creation of two photons in the subharmonic mode due to the loss of a single photon in the pump mode, and the reverse interaction is also present. The strength of this interaction is determined by the parameter g.

The fourth term in Equation (3.84) represents the source of the new pump mode. The pump mode arises due to pumping applied to the system at the frequency $2\omega_0$. This can be seen as analogous to a driving force applied to a classical oscillator forcing the oscillator to oscillate at that driving frequency. For a more in depth discussions of the source of these terms in the Hamiltonian, see [10] and [13].

Because the changes predominantly take place in H_S, the derivation in Section 3.7.3 is mostly the same. The only difference comes from the extra set of b terms in H_{SR}. These just lead to the repetition of the damping terms in Equation (3.83) but for b. The extra terms in H_S are ignored after transforming into the interaction picture, and then return as Hamiltonian terms in Equation (3.83). The master equation for the degenerate parametric oscillator is

$$\begin{aligned}\dot{\rho} &= \frac{1}{i\hbar}[H_{ab}+H_{drive},\rho]+(\rho)_a+(\rho)_b \\ &= -i\omega_0[a^\dagger a,\rho]-2i\omega_0[b^\dagger b,\rho]+\frac{g}{2}[a^{\dagger 2}b-a^2b^\dagger,\rho]-i[\mathcal{E}_0e^{-i2\omega_0 t}a^{\dagger 2}+\mathcal{E}_0^*e^{i2\omega_0 t}a^2,\rho] \\ &+\frac{\gamma}{2}\bar{n}(2a^\dagger\rho a-aa^\dagger\rho-\rho aa^\dagger)+\frac{\gamma}{2}(\bar{n}+1)(2a\rho a^\dagger-a^\dagger a\rho-\rho a^\dagger a) \\ &+\frac{\gamma_p}{2}\bar{n}_p(2b^\dagger\rho b-bb^\dagger\rho-\rho bb^\dagger)+\frac{\gamma_p}{2}(\bar{n}_p+1)(2b\rho b^\dagger-b^\dagger b\rho-\rho b^\dagger b).\end{aligned} \tag{3.87}$$

where γ_p and $\bar{n}_p$ are the same as γ and $\bar{n}$ but then with respect to the pump mode's reservoir.

3.7.5. Elimination of pump mode

Equation (3.87) consists of different operators acting on the state ρ, however it is still longer than desired. In order to arrive at the master equation for the van der Pol oscillator, the pump mode will be traced out, similar to how the reservoir was traced out in the previous sections. For this subsection, superoperator notation is used in which rather than writing $a\rho a^\dagger$ (for example), the notation $(a\cdot a^\dagger)\rho$ is written. This also means later superoperators can be evaluated such as $(a\cdot)(\cdot a^\dagger)\rho=(a\cdot a^\dagger)\rho$. Equation (3.87) is transformed into the interaction picture with $H_0=\omega_0a^\dagger a+2\omega_0b^\dagger b+\mathcal{E}_0e^{-i2\omega_0 t}b^\dagger+\mathcal{E}_0^*e^{i2\omega_0 t}b$, meaning that those terms can be left out of the master equation for $\tilde{\rho}=e^{iH_{0,S}t/\hbar}\rho e^{-iH_{0,S}t/\hbar}$. This follows from Equation (3.47), with the effect of internal interactions on reservoir interaction being neglected [13]. A final note is that the assumption $\bar{n}_p=0$ is made i.e, the average number of photons in the reservoir with which the pump mode exchanges photons is zero [13]. The equation for $\tilde{\rho}$ can be written as

$$\dot{\tilde{\rho}}=(\mathcal{L}_s+\mathcal{L}_p+\mathcal{L}_{sp})\tilde{\rho}, \tag{3.88}$$

with

$$\mathcal{L}_s\equiv\frac{\gamma}{2}\bar{n}(2a^\dagger\cdot a-aa^\dagger\cdot-\cdot aa^\dagger)+\frac{\gamma}{2}(\bar{n}+1)(2a\cdot a^\dagger-a^\dagger a\cdot-\cdot a^\dagger a), \tag{3.89}$$

$$\mathcal{L}_p\equiv\frac{\gamma_p}{2}(2b\cdot b^\dagger-b^\dagger b\cdot-\cdot b^\dagger b), \tag{3.90}$$

$$\mathcal{L}_{sp}\equiv\frac{g}{2}[a^{\dagger 2}b-a^2b^\dagger,\ \cdot\ ]. \tag{3.91}$$

Equation (3.88) consists of three different superoperators acting on $\tilde{\rho}$, one representing just the subharmonic terms, one just the pump terms, and one describing the interaction between the two modes. This is similar to how in Equation (3.47) a transformation was made to isolate H_{SR} from H_S and H_R, here the transformation is made to isolate the interaction between the subharmonic and the pump:

$$\bar{\rho}(t) \equiv e^{-(\mathcal{L}_s+\mathcal{L}_p)t}\tilde{\rho}(t)e^{(\mathcal{L}_s+\mathcal{L}_p)t}, \tag{3.92}$$

$$\bar{\mathcal{L}}_{sp}(t) \equiv e^{-(\mathcal{L}_s+\mathcal{L}_p)t}\mathcal{L}_{sp}e^{(\mathcal{L}_s+\mathcal{L}_p)t}, \tag{3.93}$$

giving the master equation

$$\dot{\bar{\rho}} = \bar{\mathcal{L}}_{sp}\bar{\rho}. \tag{3.94}$$

The desired density matrix is the one for the subharmonic, which is found by tracing out the pump:

$$\bar{\sigma}(t) \equiv Tr_p[\bar{\rho}(t)]. \tag{3.95}$$

In a similar fashion to Section 2.1, Equation (3.94) is integrated once, then substituted back into itself, and then the trace is taken to arrive at the following equation of motion for $\bar{\sigma}$:

$$\dot{\bar{\sigma}} = Tr_p[\bar{\mathcal{L}}_{sp}(t)\rho(0)] + \int_0^t tr_p[\bar{\mathcal{L}}_s p(t)\bar{\mathcal{L}}_{sp}(t'\bar{\rho}(t')]dt'. \tag{3.96}$$

The first term can be removed by assuming the pump mode is (to approximation) in the vacuum state ($\langle 0|0\rangle$) [13]. This means the ansatz can be introduced: $\bar{\rho}(t) = \bar{\sigma}(t)(\langle 0|0\rangle)$.

Using the properties of superoperators, $\bar{\mathcal{L}}_{sp}(t)$ can be evaluated:

$$\begin{aligned}\bar{\mathcal{L}}_{sp}(t) &= \frac{g}{2}e^{-(\mathcal{L}_s+\mathcal{L}_p)t}[(a^{\dagger 2}\cdot)(b\cdot) - (a^2\cdot)(b^\dagger\cdot) - (a^2\cdot)^\dagger(b^\dagger\cdot)^\dagger + (a^{\dagger 2}\cdot)^\dagger(b\cdot)^\dagger]e^{(\mathcal{L}_s+\mathcal{L}_p)t} \\ &= \frac{g}{2}[\bar{\mathcal{S}}_1(t)\bar{\mathcal{P}}_1(t) - \bar{\mathcal{S}}_2(t)\bar{\mathcal{P}}_2(t) + \bar{\mathcal{S}}^\dagger{}_1(t)\bar{\mathcal{P}}^\dagger{}_1(t) - \bar{\mathcal{S}}_2^\dagger(t)\bar{\mathcal{P}}_2^\dagger(t)],\end{aligned} \tag{3.97}$$

with

$$\bar{\mathcal{S}}_1(t) \equiv e^{-\mathcal{L}_s t}(a^{\dagger 2}\cdot)e^{\mathcal{L}_s t}, \tag{3.98}$$

$$\bar{\mathcal{S}}_2(t) \equiv e^{-\mathcal{L}_s t}(a^2\cdot)e^{\mathcal{L}_s t}, \tag{3.99}$$

$$\begin{aligned}\bar{\mathcal{P}}_1(t) &\equiv e^{-\mathcal{L}_p t}(b\cdot)e^{\mathcal{L}_p t} \\ &= e^{-(\gamma_p/2)t}(b\cdot),\end{aligned} \tag{3.100}$$

$$\begin{aligned}\bar{\mathcal{P}}_2(t) &\equiv e^{-\mathcal{L}_p t}(b^\dagger\cdot)e^{\mathcal{L}_p t} \\ &= e^{(\gamma_p/2)t}(b^\dagger\cdot) + (e^{-(\gamma_p/2)t} - e^{(\gamma_p/2)t})(\cdot b^\dagger).\end{aligned} \tag{3.101}$$

Equations (3.100) and (3.101) are derived in Appendix A.3. Now all that is left is substituting these equations into Equation (3.96) and evaluating terms. Many terms vanish due to the assumption that the pump mode is in the vacuum state:

$$\bar{\mathcal{L}}_{sp}(t)\bar{\sigma}(t')(|0\rangle\langle 0|)_p = -\left(\frac{g}{2}\right)e^{\kappa_p t'}[\bar{\mathcal{S}}_2(t')(b^\dagger\cdot) + \bar{\mathcal{S}}_2^\dagger(t')(\cdot b)]\bar{\sigma}(t')(|0\rangle\langle 0|)_p, \tag{3.102}$$

where $\kappa_p = \frac{\gamma_p}{2}$.

This gives:

$$
\begin{aligned}
\bar{\mathcal{L}}_{sp}(t)\bar{\mathcal{L}}_{sp}(t')\bar{\sigma}(t')(|0\rangle\langle 0|)_p &= -\left(\frac{g}{2}\right)^2 e^{\kappa_p t'}\left(\bar{\mathcal{S}}_1(t)\bar{\mathcal{P}}_1(t) - \bar{\mathcal{S}}_2(t)\bar{\mathcal{P}}_2(t) + \bar{\mathcal{S}}^\dagger{}_1(t)\bar{\mathcal{P}}^\dagger{}_1(t) - \bar{\mathcal{S}}_2^\dagger(t)\bar{\mathcal{P}}_2^\dagger(t)\right) \\
&\cdot [\bar{\mathcal{S}}_2(t')(b^\dagger\cdot) + \bar{\mathcal{S}}_2^\dagger(t')(\cdot b)]\bar{\sigma}(t')(|0\rangle\langle 0|)_p \\
&= -\left(\frac{g}{2}\right)^2 e^{\kappa_p t'}[e^{-\kappa_p t}\bar{\mathcal{S}}_1(t)(b\cdot) - e^{\kappa_p t}\bar{\mathcal{S}}_2(t)(b^\dagger\cdot) - (e^{-\kappa_p t} - e^{\kappa_p t})\bar{\mathcal{S}}_2(t)(\cdot b^\dagger) \\
&+ \bar{\mathcal{S}}^\dagger{}_1(t)e^{-\kappa_p t}(\cdot b^\dagger) - e^{\kappa_p t}\bar{\mathcal{S}}_2^\dagger(t)(\cdot b) - (e^{-\kappa_p t} - e^{\kappa_p t}\bar{\mathcal{S}}_2^\dagger(b\cdot)] \\
&\cdot \left(\bar{\mathcal{S}}_2(t')(b^\dagger\cdot) + \bar{\mathcal{S}}_2^\dagger(\cdot b)\right)\bar{\sigma}(t')(|0\rangle\langle 0|)_p \\
\\
&= -\left(\frac{g}{2}\right)^2 \Big[[e^{\kappa_p(t'-t)}\bar{\mathcal{S}}_1(t)\bar{\mathcal{S}}_2(t')(bb^\dagger\cdot) - e^{\kappa_p(t'+t)}\bar{\mathcal{S}}_2(t)\bar{\mathcal{S}}_2(t')(b^{\dagger 2}\cdot) \\
&- e^{\kappa_p(t'+t)}\bar{\mathcal{S}}^\dagger{}_2(t)\bar{\mathcal{S}}_2(t')(b^\dagger\cdot b) - (e^{\kappa_p(t'-t)} - e^{\kappa_p(t'+t)})\bar{\mathcal{S}}^\dagger{}_2(t)\bar{\mathcal{S}}_2(t')(bb^\dagger\cdot) \\
&- e^{\kappa_p(t'+t)}\bar{\mathcal{S}}_2(t)\bar{\mathcal{S}}^\dagger{}_2(t')(b^\dagger\cdot b) - (e^{\kappa_p(t'-t)} - e^{\kappa_p(t'+t)})\bar{\mathcal{S}}_2(t)\bar{\mathcal{S}}^\dagger{}_2(t')(\cdot bb^\dagger) \\
&+ e^{\kappa_p(t'-t)}\bar{\mathcal{S}}^\dagger{}_1(t)\bar{\mathcal{S}}^\dagger{}_2(t')(\cdot bb^\dagger) - e^{\kappa_p(t'+t)}\bar{\mathcal{S}}^\dagger{}_2(t)\bar{\mathcal{S}}^\dagger{}_2(t')(\cdot b^2)\Big]\bar{\sigma}(t')(|0\rangle\langle 0|)_p \qquad (3.103) \\
\\
&= -\left(\frac{g}{2}\right)^2 e^{\kappa_p(t'-t)}\Big[\bar{\mathcal{S}}_1(t)\bar{\mathcal{S}}_2(t')(bb^\dagger\cdot) - \bar{\mathcal{S}}^\dagger{}_2(t)\bar{\mathcal{S}}_2(t')(bb^\dagger\cdot) \\
&\qquad - \bar{\mathcal{S}}_2(t)\bar{\mathcal{S}}^\dagger{}_2(t')(\cdot bb^\dagger) + \bar{\mathcal{S}}^\dagger{}_1(t)\bar{\mathcal{S}}^\dagger{}_2(t')(\cdot bb^\dagger)\Big]\bar{\sigma}(t')(|0\rangle\langle 0|)_p \\
&\quad -\left(\frac{g}{2}\right)^2 e^{\kappa_p(t'+t)}\Big[- \bar{\mathcal{S}}_2(t)\bar{\mathcal{S}}_2(t')(b^{\dagger 2}\cdot) - \bar{\mathcal{S}}^\dagger{}_2(t)\bar{\mathcal{S}}_2(t')(b^\dagger\cdot b) \\
&\qquad + \bar{\mathcal{S}}^\dagger{}_2(t)\bar{\mathcal{S}}_2(t')(bb^\dagger\cdot) - \bar{\mathcal{S}}_2(t)\bar{\mathcal{S}}^\dagger{}_2(t')(b^\dagger\cdot b) \\
&\qquad + \bar{\mathcal{S}}_2(t)\bar{\mathcal{S}}^\dagger{}_2(t')(\cdot bb^\dagger) - \bar{\mathcal{S}}^\dagger{}_2(t)\bar{\mathcal{S}}^\dagger{}_2(t')(\cdot b^2)\Big]\bar{\sigma}(t')(|0\rangle\langle 0|)_p.
\end{aligned}
$$

Before tracing, there are two types of terms, those proportional to $e^{-(\gamma_p/2)(t-t')}$ and those proportional to $e^{(\gamma_p/2)(t+t')}$. The second type seem divergent, however they vanish when the trace is taken. This is because in the square brackets the first and last terms acting on the vacuum state lead to 0, while the second and third term cancel each other out and so do the fourth and fifth terms.

The terms proportional to $e^{-(\kappa_p)(t-t')}$ type can be evaluated by approximating the exponential as a delta function : $e^{-(\kappa_p)(t-t')} \to \frac{1}{\kappa_p}\delta(t-t')$and taking the time integral in the adiabatic limit. Then writing the $\bar{\mathcal{S}}$ terms explicitly leads to the following equation of motion:

$$
\begin{aligned}
\dot{\bar{\sigma}} &= -\left(\frac{g}{2}\right)^2 \frac{1}{\kappa_p} e^{-\mathcal{L}_s t}\left[(a^{\dagger 2}\cdot)(a^2\cdot) - (\cdot a^\dagger 2)(a^2\cdot) - (a^2\cdot)(\cdot a^\dagger 2 + (\cdot a^2)(\cdot a^{\dagger 2})\right] e^{\mathcal{L}_s t}\bar{\sigma} \\
&= \frac{g^2}{2\gamma_p} e^{-\mathcal{L}_s t}[2(a^2\cdot a^{\dagger 2}) - (a^{\dagger 2}a^2\cdot) - (\cdot a^{\dagger 2}a^2)]e^{\mathcal{L}_s t}\bar{\sigma}. \qquad (3.104)
\end{aligned}
$$

Now all that is left to be done is to invert some of the transformations made. The transformations corresponding to H_S and $\mathcal{L}_s$ are inverted, however the transformation due to the driving term is left in so this does not appear in the master equation. Writing $\sigma(t) = e^{-i\omega_0 a^\dagger a t}[e^{\mathcal{L}_s t}\bar{\sigma}(t)e^{-\mathcal{L}_s t}]e^{i\omega_0 a^\dagger a t}$, this leads to

$$
\begin{aligned}
\dot{\sigma} &= -i[\omega_0 a^\dagger a, \sigma] + \frac{\gamma}{2}\bar{n}(2a^\dagger\sigma a - aa^\dagger\sigma - \sigma aa^\dagger) + \frac{\gamma}{2}(\bar{n}+1)(2a\sigma a^\dagger - a^\dagger a\sigma - \sigma a^\dagger a) \\
&\quad + \frac{g^2}{2\gamma_p}[2(a^2\sigma a^{\dagger 2}) - (a^{\dagger 2}a^2\sigma) - (\sigma a^{\dagger 2}a^2)] \qquad (3.105) \\
&= -\frac{i}{\hbar}[H_a, \sigma] + \gamma\bar{n}\mathcal{D}[a^\dagger](\sigma) + \gamma(\bar{n}+1)\mathcal{D}[a](\sigma) + \frac{g^2}{\gamma_p}\mathcal{D}[a^2](\sigma).
\end{aligned}
$$

This equation is very similar to Equation (3.35) however there is a $\mathcal{D}[a](\sigma)$ which is not present in the master equation for the quantum van der Pol oscillator commonly studied [3][4][7][14]. As noted in [15], this is resolved by combining the negative linear damping and the normal linear damping into one physical process.

In the next chapter quantum van der Pol oscillators following Equation (3.35) will be coupled in a variety of systems to study their synchronisation behaviour based on the coupling strengths and frequency differences.

4

Quantum synchronisation

Now that the foundations have been laid for the description of oscillatory behaviour in quantum systems with dissipation, the synchronisation in these systems will be investigated. This chapter will first return to the first classical discrete model described in this paper, and discuss how this can be extended to include quantum mechanical behaviour as done in [6]. Then the synchronisation of coupled quantum van der Pol oscillators will be investigated, the results of which will be presented in Chapter 5.

4.1. Simple quantum synchronisation model

To extend the model of Equations (2.4)-(2.7) to the quantum case, the equations first have to be written in terms of states and operators. Instead of writing θ_t and ϕ_t seperately, the total state is written as $|\psi_t\rangle = |\theta_t\rangle \otimes |\phi_t\rangle$ where $|\theta_t\rangle$ and $|\phi_t\rangle$ are vectors from the basis $\{|i\rangle\}_{i=0}^{d-1}$, with d the dimension of the model.

Two new operators are defined:

$$\hat{\theta} = \left(\sum_{i=1}^{d-1} i|i\rangle\langle i|\right) \otimes \hat{\mathbb{1}}, \quad \hat{\phi} = \hat{\mathbb{1}} \otimes \left(\sum_{i=1}^{d-1} i|i\rangle\langle i|\right), \tag{4.1}$$

allowing one to obtain the values $\theta_t = \langle\psi_t|\hat{\theta}|\psi_t\rangle$ and $\phi_t = \langle\psi_t|\hat{\phi}|\psi_t\rangle$ from the state.

The rotations can be described by the following operators:

$$\hat{U}_\Omega|\theta_t\rangle = |\theta_t + \Omega \pmod d\rangle, \quad \hat{U}_\omega|\phi_t\rangle = |\phi_t + \omega \pmod d\rangle. \tag{4.2}$$

Until now there have not been any significant differences between this model and the original model in Equations (2.4)-(2.7). Suppose the following operator was introduced to perform the coupling, performing the same action on the system as Equation (2.7):

$$\hat{G}_K|\theta_t\rangle \otimes |\phi_t\rangle = \begin{cases} |\theta_t\rangle \otimes |\theta_t\rangle, & \text{if } |\Delta_t| \leq K, \\ |\theta_t\rangle \otimes |\phi_t\rangle, & \text{otherwise,} \end{cases} \tag{4.3}$$

again taking Δ_t such that $\Delta_t \bmod d$ is minimised.

Then one time step can be described by

$$|\psi_{t+1}\rangle = (\hat{U}_\Omega \otimes \hat{U}_\omega)\hat{G}_K|\psi_t\rangle. \tag{4.4}$$

This model works very well for systems described in the original model where θ_t and ϕ_t have single values, however in the quantum model, $|\theta_t\rangle$ and $|\phi_t\rangle$ can be in a superposition. Suppose the transformation $\hat{G}_K$ (with $K = 2$) is performed on the state $|0\rangle \otimes \left(\frac{1}{\sqrt{2}}|0\rangle + \frac{1}{\sqrt{2}}|1\rangle\right)$ such that $|\phi_t\rangle$ is in a superposition. Each part of the superposition is transformed independently leading to the new state $\frac{2}{\sqrt{2}}|0\rangle \otimes |0\rangle$. This state is clearly non-physical, as the total probability is no longer 1.

Here the difficulties of converting a classical model to a quantum model is again observed. This time the problem lies in the operator $\hat{G}_K$, which is not a reversible process, and so it is not a unitary transformation.

This problem is similar to the problem discussed in Section 3.3, where the simple introduction of a damping term led to an irreversible process.

Nevertheless $\hat{G}_K$ can be adjusted such that the transformation is reversible. This is done by introducing an ancillary system with basis vectors $\{|\bar{0}\rangle\} \cup \{|i\rangle\}_{i=0}^{d-1}$ and introducing the unitary operator $\hat{V}_K$. $|\bar{0}\rangle$ is the state to which the ancilla is reset after each iteration. The operator is defined as follows:

$$\hat{V}_K|\theta_t\rangle \otimes |\phi_t\rangle \otimes |\bar{0}\rangle = \begin{cases} |\theta_t\rangle \otimes |\theta_t\rangle \otimes |\bar{0}\rangle, & \text{if } \Delta_t = 0, \\ |\theta_t\rangle \otimes |\phi_t\rangle \otimes |\bar{0}\rangle, & \text{if } |\Delta_t| \geq K, \\ |\theta_t\rangle \otimes |\theta_t\rangle \otimes |\Delta_t\rangle, & \text{otherwise.} \end{cases} \tag{4.5}$$

By taking into account Δ_t during the transformation, the operator is reversible even when performed onto states that are in a superposition. After every time step the ancilla is reset to $\bar{0}$. It is this action that is the source of dissipation, an important feature that allows synchronisation to occur. This action is peformed by replacing the state $|\psi_t\rangle$ by a density matrix ρ_t, such that the ancilla can be traced out after every time step. The time evolution is described by the following equations:

$$\theta_{t+1} = \mathrm{Tr}\{\rho_{t+1}\hat{\theta}\}, \tag{4.6}$$

$$\phi_{t+1} = \mathrm{Tr}\{\rho_{t+1}\hat{\phi}\}, \tag{4.7}$$

$$\Delta_{t+1} = \mathrm{Tr}\{\rho_{t+1}(\hat{\theta} - \hat{\phi})\}, \tag{4.8}$$

where

$$\rho_{t+1} = \mathrm{Tr}_{anc}\left\{\hat{\mathbb{U}}(\rho_t \otimes |\bar{0}\rangle\langle\bar{0}|_{anc}\hat{\mathbb{U}}^\dagger\right\}, \tag{4.9}$$

and

$$\hat{\mathbb{U}} = (\hat{U}_\Omega \otimes \hat{U}_\omega \otimes \mathbb{1})\hat{V}_K. \tag{4.10}$$

This model is able to reproduce results similar to those presented in Figure 2.2, while allowing for superpositions of states.

A slightly different model makes it possible to investigate the synchronisation of a single qubit. A qubit refers to a quantum mechanical system with two levels, so in this model it refers to the system with $d = 2$.

4.1.1. Synchronisation of a single qubit

By adjusting the model to one in which a qubit is driving by a single oscillator, the conditions for phase locking can be deduced. Now ϕ_t is restricted to taking on the values $0, 1$ while θ_t can still take values up to d. The rotation of the qubit is described by the following operator:

$$\hat{R}^n\begin{pmatrix}|0\rangle\\|1\rangle\end{pmatrix} = \begin{pmatrix}\cos\frac{n\pi}{d} & \sin\frac{n\pi}{d}\\ -\sin\frac{n\pi}{d} & \cos\frac{n\pi}{d}\end{pmatrix}\begin{pmatrix}|0\rangle\\|1\rangle\end{pmatrix}. \tag{4.11}$$

This operator can be seen as a rotation of the qubit on the Bloch sphere by an angle $\frac{2n\pi}{d}$ about the y axis. The exponent n indicates how many times a rotation of $\frac{2\pi}{d}$ is applied to the qubit.

The coupling transformation has the form

$$\hat{W}_K|\theta_t\rangle \otimes |\phi_t\rangle \otimes |0\rangle = \begin{cases} |\theta_t\rangle \otimes |\phi_t\rangle \otimes |0\rangle, & \text{if } |\theta_t - \frac{d}{2}\phi_t| > K, \\ |\theta_t\rangle \otimes \hat{R}^{\theta_t}|0\rangle \otimes |1\rangle, & \text{otherwise,} \end{cases} \tag{4.12}$$

which when the requirement is satisfied, will rotate the qubit based on the value of θ_t. The time evolution is described by

$$\rho_{t+1} = \mathrm{Tr}_{anc}\left\{\hat{\mathbb{Q}}(\rho_t \otimes |\bar{0}\rangle\langle\bar{0}|_{anc}\hat{\mathbb{Q}}^\dagger\right\}, \tag{4.13}$$

and

$$\hat{\mathbb{Q}} = (\hat{U}_\Omega \otimes \hat{R}^\omega \otimes \mathbb{1})\hat{W}_K. \tag{4.14}$$

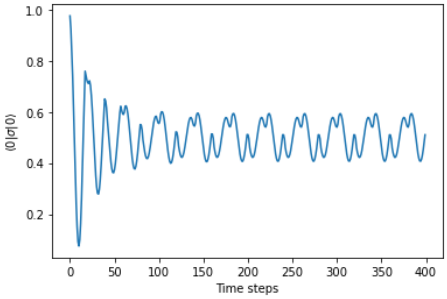

(a) Numerical simulation with $\Omega = 1$, $\omega = 2$, $K = 2$. Phase locking occur causing the qubit to oscillate with frequency $\Omega = 1$ with a period of $\frac{d}{\Omega} = 40$.

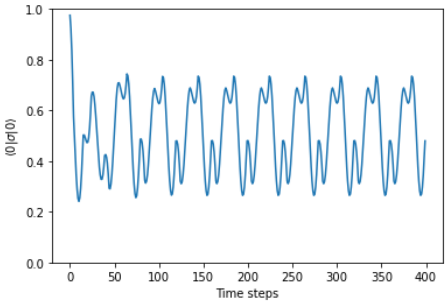

(b) Numerical simulation with $\Omega = 1$, $\omega = 2$, $K = 4$. Just as in (a), phase locking occurs with qubit oscillating at the same frequency. However because K is larger, phase locking occurs earlier allowing the qubit to maintain a more pure state while oscillating.

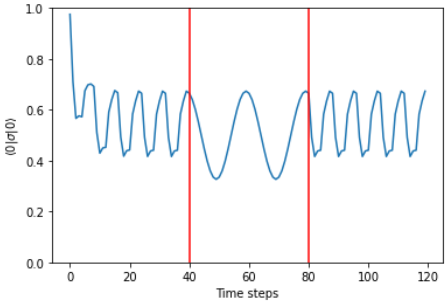

(c) Numerical simulation with $\Omega = 5$, $\omega = 2$, $K = 5$, but between $n = 40$ and $n = 80$ the interaction is turned off causing the qubit to return to its own frequency.

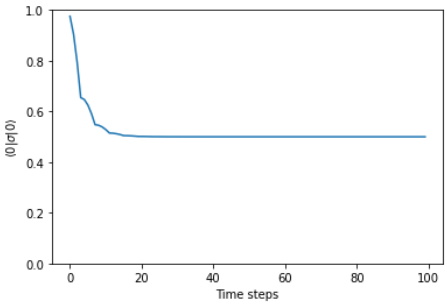

(d) Numerical simulation with $\Omega = 5$, $\omega = 2$, $K = 3$. Here the qubit evolves into a maximally mixed state.

Figure 4.1: Numerical simulations for the state of the qubit evaluated using Equation (4.14) for $d = 40$ and different parameters for Ω, ω and k (see subcaptions). The y-axis shows $\langle 0|\sigma|0\rangle$ with σ being the density matrix of the qubit. The qubit has initial state $\sigma = |0\rangle\langle 0|$. Although the model is discrete, the points have been connected for clarity. Phase locking can be observed in figures (a)-(c) where after a certain number of time steps, the qubit begins to oscillate with the frequency of the stimulus as opposed to its own frequeny.

An alternate description for how this model evolves can be found in [6]. The behaviour displayed by this model can be investigated by looking at $\langle 0|\sigma_t|0\rangle$ where σ_t is the density matrix of the qubit. Figure 4.1 shows some examples of the behaviour of this model.

In the case that there exists values of t such that $|\Omega t| \leq K$ or $|\Omega t - \frac{d}{2}| \leq K$, phase locking will occur. In Figure 4.1a this occurs after approximately 100 time steps, causing the qubit to oscillate with the frequency of the stimulus. In Figure 4.1b, slightly different behaviour is observed as K is increased allowing phase locking to occur earlier and with the qubit in a more pure state. Figure 4.1c shows that when the interaction between the stimulus and the qubit is turned off, the qubit will return to its own frequency. After turning the interaction back on, the qubit phase locks with stimulus again.

In the case that the interaction only occurs for values t such that $\theta_t = 0, \frac{d}{2}$, behaviour as displayed in Figure 4.1d is observed where the qubit evolves into a maximally mixed state. Here the purity defined in Equation (3.8) is $\frac{1}{2}$ which is the minimal value. This is because for these two values of θ_t, the operator $\hat{W}_K$ essentially measures the state of the qubit in the $\{|0\rangle, |1\rangle\}$ basis, causing the length of the qubit's Bloch vector to decrease and eventually causing the qubit to become maximally mixed.

In this section, the classical model described in Section 2.2 was further developed into a quantum model. In the process, certain challenges were discussed concerning quantum behaviour, and how they could be met. The behaviour of such a quantum model was then discussed in terms of attempting to synchronise a qubit. In the next section, the synchronisation of quantum van der Pol oscillators will be investigated and the possibilities of synchronising the systems of quantum van der Pol oscillators displayed in Figure 2.5.

4.2. Synchronisation of quantum van der Pol oscillators

A single quantum van der Pol oscillator follows Equation (3.35). Two quantum van der Pol oscillators can be synchronised by coupling them to one another. This coupling can take two forms: reactive coupling and

dissipative coupling. Reactive coupling occurs by introducing a $H = V(a_1 a_2^\dagger + a_1^\dagger a_2)$ to the Hamiltonian , with a_1, a_2 being the annihilation operators for the first and second oscillator respectively, as in Equation (3.32). This type of coupling was studied in [3]. This thesis will focus on dissipative coupling which is implemented by introducing a Lindbladian term $\mathcal{D}[a_1 - a_2](\rho)$ [4].

4.2.1. Two coupled quantum van der Pol oscillators

Two dissipatively coupled quantum van der Pol oscillators with identical damping have the following master equation:

$$\dot{\rho} = -i[H,\rho] + V\mathcal{D}[a_1 - a_2](\rho) + \sum_{k=1}^{2} \gamma_\downarrow \mathcal{D}[\hat{a}_k^2](\rho) + \gamma_\uparrow \mathcal{D}[\hat{a_k}^\dagger](\rho), \tag{4.15}$$

where $H = \omega_1 \hat{a}_1^\dagger \hat{a}_1 + \omega_2 \hat{a}_2^\dagger \hat{a}_2$ and V is the strength of the coupling. The density matrix ρ describes the state of the total system including both oscillators. Note that in the Hamiltonian, $\hbar$ has been set to 1.

This thesis will not address the three coupled quantum van der Pol oscillators, the study of which can be found in [5].

4.2.2. Four coupled quantum van der Pol oscillators

The master equations for four coupled quantum van der Pol oscillators with identical damping all have a similar form to Equation (4.15) : the normal Hamiltonian term, the negative and non-linear damping terms for each oscillator, and a coupling term proportional to V for each connection between two oscillators. As a result they all take the form of

$$\dot{\rho} = -i[H,\rho] + \sum_{k=1}^{4} \gamma_\downarrow \mathcal{D}[\hat{a}_k^2](\rho) + \gamma_\uparrow \mathcal{D}[\hat{a_k}^\dagger](\rho) + V \sum_{j=1}^{4} \sum_{k=j+1}^{4} c_{j,k} \mathcal{D}[\hat{a}_j - \hat{a}_k]\rho], \tag{4.16}$$

where $H = \omega_1 \hat{a}_1^\dagger \hat{a}_1 + \omega_2 \hat{a}_2^\dagger \hat{a}_2 + \omega_3 \hat{a}_3^\dagger \hat{a}_3 + \omega_4 \hat{a}_4^\dagger \hat{a}_4$, and $c_{j,k}$ determines whether there is a connection or not given by

$$c_{j,k} = \begin{cases} 1 & \text{if there is a connection between oscillators } j \text{ and } k, \\ 0 & \text{otherwise.} \end{cases} \tag{4.17}$$

The second summation is only from $j+1$ to 4 because for a single coupling between two oscillators to be present there is no need to include both directions of the coupling. As an example, for the chain system the master equation is

$$\dot{\rho} = -i[H,\rho] + \sum_{k=1}^{4} \left[\gamma_\downarrow \mathcal{D}[\hat{a}_k^2](\rho) + \gamma_\uparrow \mathcal{D}[\hat{a_k}^\dagger] \right] + V \left(\mathcal{D}[\hat{a}_2 - \hat{a}_1](\rho) + \mathcal{D}[\hat{a}_3 - \hat{a}_2](\rho) + \mathcal{D}[\hat{a}_4 - \hat{a}_3](\rho) \right). \tag{4.18}$$

The values of $c_{j,k}$ for each system is shown in Table 4.1:

Table 4.1: Table indicating where a coupling is present for each of the 4 coupled oscillator systems.

	Tree	Chain	Loop	Tower	Spade	All-to-all
$c_{1,2}$	1	1	1	1	1	1
$c_{1,3}$	1	0	0	1	1	1
$c_{1,4}$	1	0	0	1	1	1
$c_{2,3}$	0	1	1	1	1	1
$c_{2,4}$	0	0	0	0	0	1
$c_{3,4}$	0	1	1	0	1	1

For the classical van der Pol oscillator, the phase could be defined by finding the amplitude equation allowing the phase difference between coupled oscillators to be determined. By determining for what parameters the phase difference could be constant, the Arnold tongues were found. However, the phases of quantum van der Pol oscillators are more difficult to compare, so determining when synchronisation occurs is more difficult. Two measures of synchronisation will be studied.

4.2.3. Synchronisation measures

The first measure that will be investigated is the complex-valued correlator [16][17]:

$$C_{\psi_{i,j}}(t) = \frac{\langle \hat{a}_i^\dagger \hat{a}_j \rangle_{\psi_{i,j}(t)}}{\sqrt{\langle \hat{a}_i^\dagger \hat{a}_i \rangle_{\psi_{i,j}(t)} \langle \hat{a}_j^\dagger \hat{a}_j \rangle_{\psi_{i,j}(t)}}}. \tag{4.19}$$

The angle of this correlator $C_{\psi_{i,j}} = |C\psi_{i,j}|e^{i\Delta\phi}$ characterises the phase difference between two oscillators. Phase locking will be strongest when $|C\psi_{i,j}| \to 1$, indicating that the phase difference is well defined. The focus of the results will be on this measurement.

The second measure relates to the von Neumann entropy defined by

$$S(\rho) = -\mathrm{Tr}(\rho \ln \rho). \tag{4.20}$$

For pure states, $\rho = \rho^2$, and substituting this into the logarithm leads to

$$S(\rho) = -\mathrm{Tr}(\rho \ln \rho^2) = -2\mathrm{Tr}(\rho \ln \rho) = 2S(\rho) \tag{4.21}$$

$$\implies S(\rho) = 0. \tag{4.22}$$

Therefore the von Neumman entropy can quantify the departure of a system from a pure state.

It can be shown that in the quantum limit, a single quantum van der Pol oscillator has a steady state of $\rho_s = \frac{2}{3}|0\rangle\langle 0| + \frac{1}{3}|1\rangle\langle 1|$ [3]. This density matrix is diagonal, and it is also a very mixed state with a purity of only 0.56. When trying to synchronise a quantum van der Pol oscillator by coupling it to other oscillators, the steady state for a single oscillator will deviate from this state and coherences (off-diagonal terms) will appear in the density matrix for the state. The measure proposed in [18] quantifies the synchronisation of a steady state by minimising the distance between this steady state and all possible limit-cycle states using the von Neumann entropy. It is shown that this minimum value, which is the measure of synchronisation, is given by

$$\Omega = S(\rho_{\mathrm{diag}}) - S(\rho), \tag{4.23}$$

where ρ is the steady state density matrix, and ρ_{diag} is found by setting all the off-diagonals terms to zero. This measure is not always valid, as it is a measure of coherence and coherence is not generally equivalent to synchronisation. The steady state of a single undriven uncoupled quantum van der Pol oscillator is diagonal, and subsequently the steady state of a system of uncoupled quantum van der Pol oscillators is also diagonal. This means that the coupling will lead to the off-diagonal terms which can be used to measure the synchronisation strength of quantum van der Pol oscillators.

With these two measures, the strength of synchronisation in different systems of coupled van der Pol oscillators can be determined. The measure in Equation (4.19) will be applied more often, however Equation (4.23) will also be investigated.

5

Results

In this chapter, the strength of synchronisation will determined for two- and four- quantum van der Pol oscillator systems. For each system discussed in Section 4.2, the steady state density matrix will be determined using the Qutip package in Python [19], for different coupling strengths and frequency differences. The measures in equations (4.19) and (4.23) will then be used to determine the strength of synchronisation. The code used to generate the figures can be found in [20].

5.1. Two coupled quantum van der Pol oscillators

Figure 5.1 shows the results for two coupled van der Pol oscillators, found by finding the steady state solutions to Equation (4.15) for different parameters.

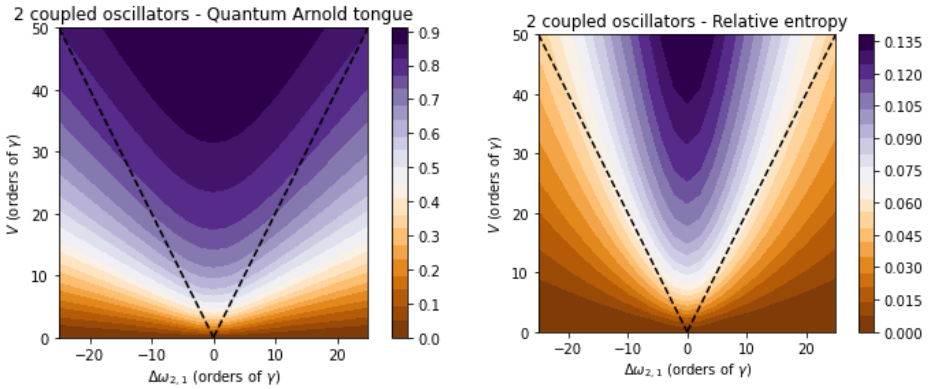

Figure 5.1: Strength of synchronisation for a 2-oscillator system determined by (a)$|C_{\psi_{1,2}}|$,(b) $S(\rho_{diag}) - S(\rho)$. The dotted line represents the classical Arnold tongue $|\Delta_{2,1}| \leq \frac{V}{2}$. $\gamma_\uparrow = 0.01, \gamma_\downarrow = 10,000$. All the axes scale with $\gamma_\uparrow$.

Figure 5.1 shows that synchronisation behaviour for the quantum van der Pol oscillators is similar to the classical case, although the synchronisation strength increases gradually rather than the system suddenly being synchronisable. There is a clear difference between the two measures of synchronisation, nevertheless they both show similarities to the classical case. This suggests the classical Arnold tongue gives a good indication of when synchronisation is likely to occur in the quantum regime.

5.2. Four coupled quantum van der Pol oscillators

The strength of synchronisation is found for each of the systems described by Equation (4.16) and Table 4.1. Figure 5.2 displays the results for $|C_{\psi_{2,1}}|$ for different values of V and $\Delta\omega_{2,1} = \Delta\omega_{3,1} = \Delta\omega_{4,1}$.

Figure 5.2 suggests a general trend of classical Arnold tongues being good estimates for the expected values of V and $\Delta\omega_{2,1}$ where the phase difference is well defined. Despite having the same classical Arnold tongue as the tree system shown in Figure 5.2a, the tower system in Figure 5.2d exhibits a higher synchronisation

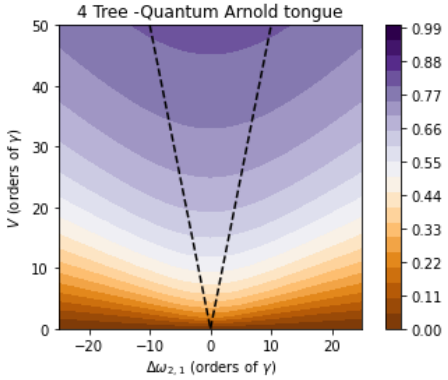

(a) Quantum Arnold tongue for the tree system. Classical arnold tongue: $|\Delta_{1,j}| \leq 0.2V$.

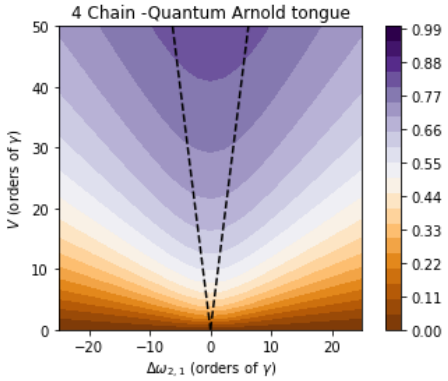

(b) Quantum Arnold tongue for the chain system. Classical arnold tongue: $|\Delta_{i,j}| \leq 0.125V$.

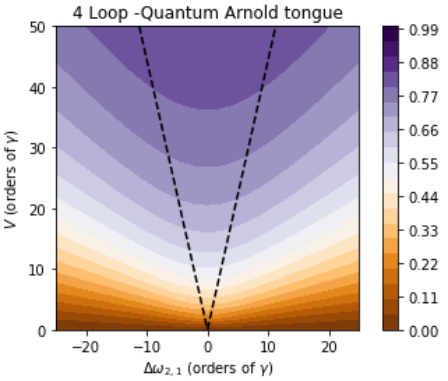

(c) Quantum Arnold tongue for the loop system. Classical arnold tongue: $|\Delta_{i,j}| \leq 0.225V$.

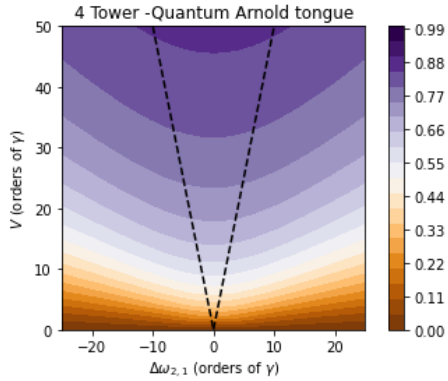

(d) Quantum Arnold tongue for the tower system. Classical arnold tongue: $|\Delta_{1,j}| \leq 0.2V$.

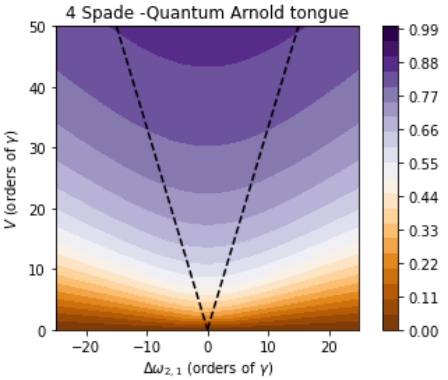

(e) Quantum Arnold tongue for the spade system. Classical arnold tongue: $|\Delta_{i,j}| \leq 0.3V$.

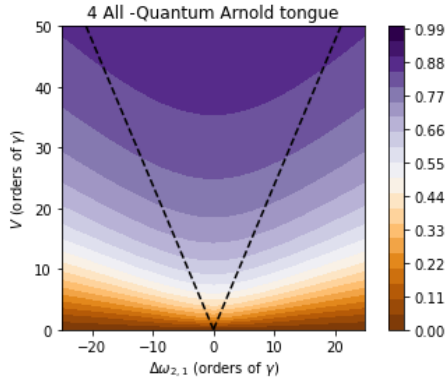

(f) Quantum Arnold tongue for the all-to-all system. Classical arnold tongue: $|\Delta_{i,j}| \leq 0.42V$.

Figure 5.2: Strength of sychronisation $|C_{\psi_{2,1}}|$, for different systems of 4 coupled quantum van der Pol oscillators. The coupling strength V increases along the y-axis while the frequency differences $\Delta\omega_{2,1} = \Delta\omega_{3,1} = \Delta\omega_{4,1}$ increases along the x-axis. The dotted line indicates the corresponding classical Arnold tongue determined in Section 2.6. $\gamma_\uparrow = 0.01$, $\gamma_\downarrow = 10000$ so the system is being studied in the quantum limit. All the axes scale with $\gamma_\uparrow$.

strength. Each of these figures only displays the correlation strength between oscillators 1 and 2 however it is interesting to see what the correlation strength is between other oscillators. These values have been determined for the chain system and are displayed in Figure 5.3. The results indicate that the strength of phase locking between oscillators that are further removed from one another is weaker. This is expected as (for example) the strength of phase locking between oscillators 1 and 3 depends on both the phase locking between oscillators 1 and 2, and oscillators 2 and 3.

Investigating systems where $\Delta\omega_{2,1} = \Delta\omega_{3,1} = \Delta\omega_{4,1}$ may lead to some discrepancy between the classical Arnold tongues and the synchronisation strength in the quantum systems, as there is no frequency difference between oscillators beyond the first. For the chain system, the classical system shows synchronisation as long as $|\Delta\omega_{2,1}| \leq 0.125V, |\Delta\omega_{3,2}| \leq 0.125V$ and $|\Delta\omega_{4,3}| \leq 0.125V$. This indicates a system that more closely follow the classical Arnold tongue would be one where each of these frequency differences are the same leading to $\Delta\omega_{4,1}$ being much larger. The results for a chain system where the frequency differences follow this trend are shown in Figure 5.4.

There is an observable symmetry present in the system, as oscillators 1 and 2 show the same correlation behaviour as oscillators 3 and 4, eventhough they are not identical. Furthermore, the correlation between oscillators 1 and 4 is weaker as their frequency difference is higher. The Arnold tongues are now also visible for the correlations between oscillators 2, 3 and 4.

The second measure of synchronisation, described by Equation (4.23) does not require any choices to be made about which oscillators are being studied. Figure 5.5 displays the results of calculating the relative entropy of synchronisation of the entire system. In general, this measure shows resemblance to the classical Arnold tongue. The relative entropy, and hence the strength of synchronisation, increases if there is more coupling present in a system. Compared to Figure 5.2, these result are actually closer to their classical counterpart, and so may be a better indication of when synchronisation is expected to occur for quantum systems. This is likely due to this measure accounting for the system as a whole, rather than measuring the correlation between only the first two oscillators.

These results have shown for what parameters phase locking is expected. The evolution of the system into a synchronised state is interesting to observe as well. Figure 5.6 shows the time evolution of $|C_{\psi_{i,j}}|$ and $\Delta\psi_{i,j}$ as it evolves into a phase locked state, for values $V = 45\gamma_\uparrow$ and $\Delta\omega_{2,1} = \Delta\omega_{3,2} = \Delta\omega_{4,3} = \gamma_\uparrow$. Synchronisation is expected to occur for these values. These figures show that the system progresses into a synchronised state quickly. They show more explicitly the difference in correlation strength between different oscillators. The correlation between oscillators 1 and 2 and the correlation between oscillators 3 and 4 tends to the same value. The symmetry in the system is visible in both the strength of the synchronisation and the phase differences between oscillators. Furthermore, the phase difference between oscillator 1 and 4 is can be determined to be the sum of the phase differences $\Delta\phi_{1.2}, \Delta\phi_{2,3}, \Delta\phi_{3,4}$. The initial behaviour of $\Delta\phi_{1,4}$ and $\Delta\phi_{3,4}$ is interesting as it increases very quickly and then decreases before following a similar trend to the other phase differences. This could be due to the chosen initial states for each oscillator. The correlation strength also exhibits interesting behaviour as it increases then decreases for each pair of oscillator before then tending toward the value at steady state. Figure 5.6c mirrors this behaviour with the strength of synchronisation being highest at an earlier time, however at steady state the synchronisation strength is lower.

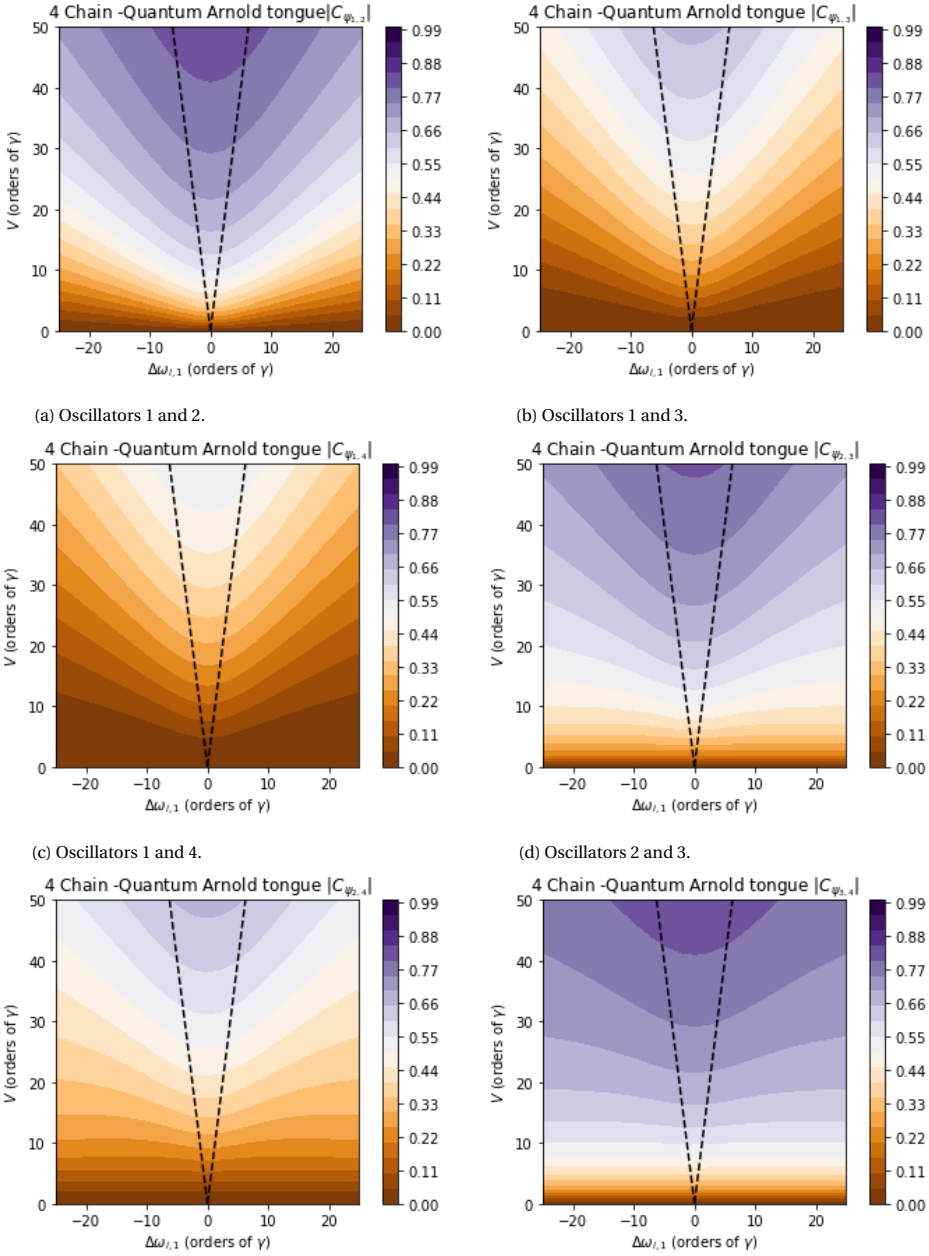

(a) Oscillators 1 and 2.

(b) Oscillators 1 and 3.

(c) Oscillators 1 and 4.

(d) Oscillators 2 and 3.

(e) Oscillators 2 and 4.

(f) Oscillators 3 and 4.

Figure 5.3: Strength of sychronisation $|C_{\psi_{i,j}}|$, between different oscillators within a system of four chain coupled quantum van der Pol oscillators. The coupling strength V increases along the y-axis while the frequency differences $\Delta\omega_{2,1} = \Delta\omega_{3,1} = \Delta\omega_{4,1}$ increases along the x-axis. The dotted line indicates the corresponding classical Arnold tongue for the classical chain system $|\Delta_{i,j}| \leq 0.125V$. $\gamma_{\uparrow} = 0.01$, $\gamma_{\downarrow} = 10000$. All the axes scale with $\gamma_{\uparrow}$.

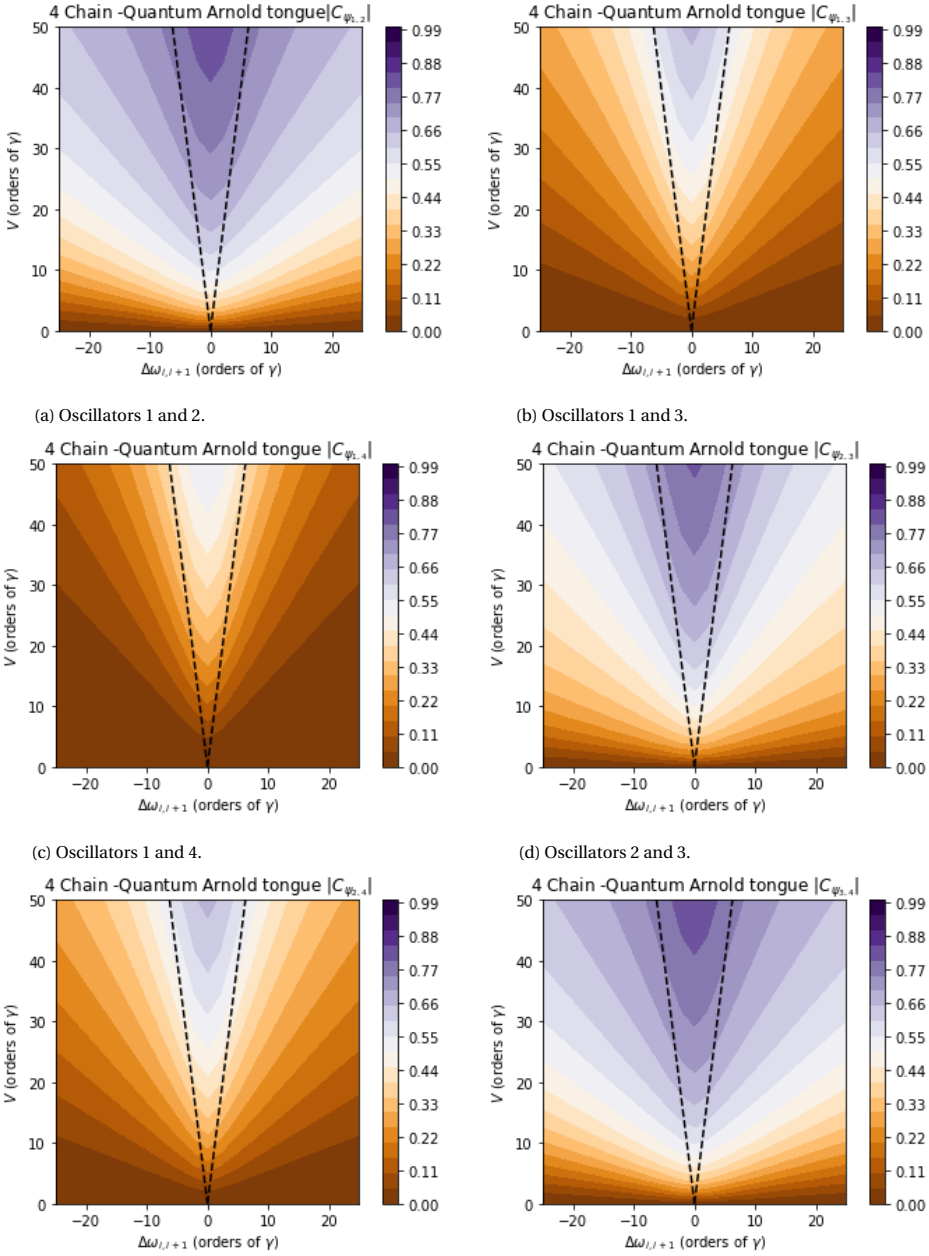

(a) Oscillators 1 and 2.

(b) Oscillators 1 and 3.

(c) Oscillators 1 and 4.

(d) Oscillators 2 and 3.

(e) Oscillators 2 and 4.

(f) Oscillators 3 and 4.

Figure 5.4: Strength of sychronisation $|C_{\psi_{i,j}}|$, between different oscillators within a system of 4 chain coupled quantum van der Pol oscillators, for different values of the coupling strength V, and the frequency difference between subsequent oscillators $\Delta\omega_{1,2} = \Delta\omega_{2,3} = \Delta\omega_{3,4}$ increases along the x-axis. The dotted line indicates the corresponding classical Arnold tongue for the classical chain system $|\Delta_{i,j}| \leq 0.25D$. $\gamma_\uparrow = 0.01$, $\gamma_\downarrow = 10000$. All the axes scale with $\gamma_\uparrow$.

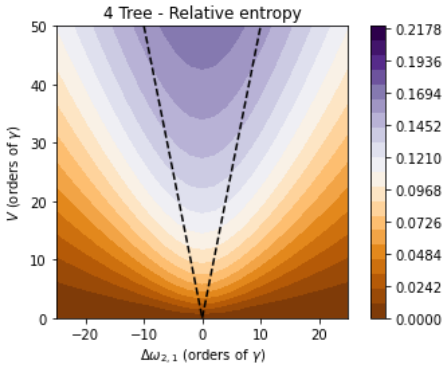

(a) Relative entropy for the tree system.
Classical Arnold tongue: $|\Delta_{1,j}| \leq 0.2V$.

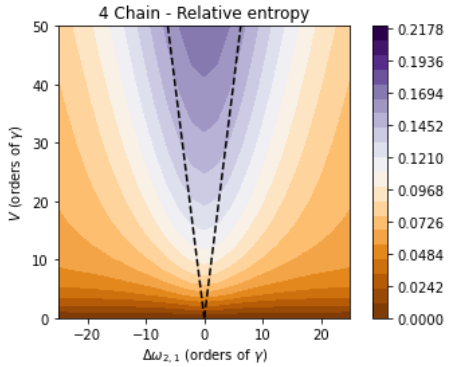

(b) Relative entropy for the chain system.
Classical Arnold tongue: $|\Delta_{i,j}| \leq 0.125V$.

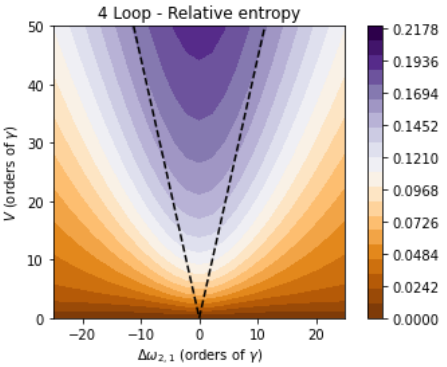

(c) Relative entropy for the loop system.
Classical Arnold tongue: $|\Delta_{i,j}| \leq 0.225V$.

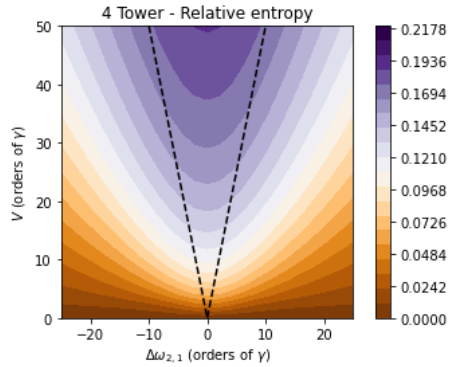

(d) Relative entropy for the tower system.
Classical Arnold tongue: $|\Delta_{1,j}| \leq 0.2V$.

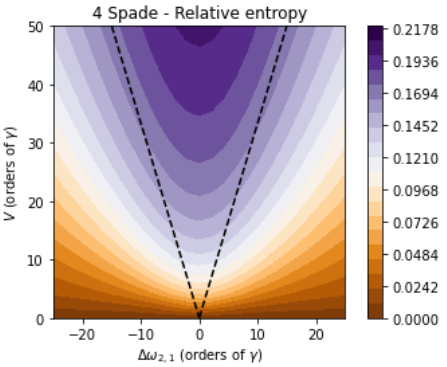

(e) Relative entropy for the spade system.
Classical Arnold tongue: $|\Delta_{i,j}| \leq 0.3V$.

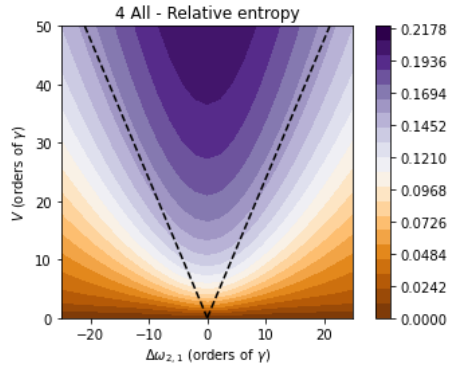

(f) Relative entropy for the all-to-all system.
Classical Arnold tongue: $|\Delta_{i,j}| \leq 0.42V$.

Figure 5.5: Strength of synchronisation determined by the relative entropy in Equation (4.23) for different systems of 4 coupled quantum van der Pol oscillators. The coupling strength V increases along the y-axis while the frequency differences $\Delta\omega_{2,1} = \Delta\omega_{3,1} = \Delta\omega_{4,1}$ increases along the x-axis. The dotted line indicates the corresponding classical Arnold tongue determined in Section 2.6. $\gamma_\uparrow = 0.01$, $\gamma_\downarrow = 10000$. All the axes scale with $\gamma_\uparrow$.

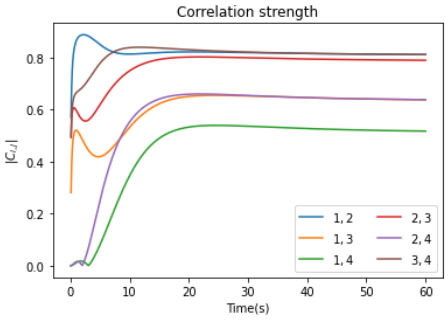

(a) Time evolution of the correlation strength between different sets of oscillators in the chain system.

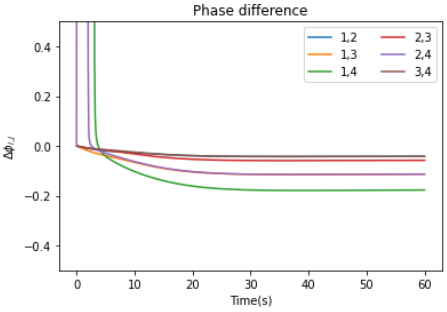

(b) Evolution of the phase differences between different sets of oscillators. The phase difference between pairs (1,2) and (3,4) initially increases to a value of almost π before decreasing, but the plot has been truncated so the behaviour of other oscillators is more visible.

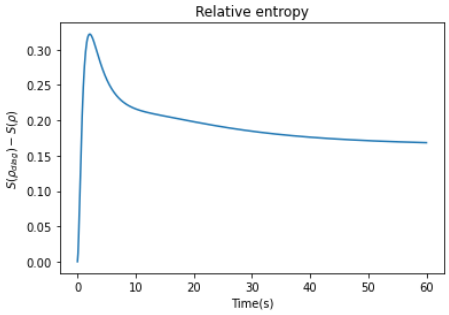

(c) Time evolution of the relative entropy of the total system.

Figure 5.6: Time evolution of the correlation, phase difference, and relative entropy between 4 chain coupled quantum van der Pol oscillators as it progresses into a synchronised steady state. $\gamma_\uparrow = 0.01$, $\gamma_\downarrow = 10000$, $V = 45\gamma_\uparrow$, $\Delta\omega_{2,1} = \Delta\omega_{3,2} = \Delta\omega_{4,3} = \gamma_\uparrow$. The system initially starts in the state $|0\rangle \otimes |1\rangle \otimes |0\rangle \otimes |1\rangle$

6

Conclusion

In this chapter, the important conclusions and results presented in the thesis will first be discussed. Subsequently, options for future research are considered.

6.1. Conclusions

This thesis has explored the behaviour of systems where synchronisation is possible. It has explored simple models for classical synchronisation and how these can be extended to allow for quantum synchronisation, focusing on systems containing four coupled quantum van der Pol oscillators. The six systems studied were the tree, chain, loop, tower, spade, and all-to-all coupled systems. Before the quantum systems were investigated, first the equivalent classical systems were explored analytically to determine for which coupling strengths and frequency differences synchronisation is expected to occur.

These synchronisation regimes (Arnold tongues) showed a number of patterns when compared to their equivalent two- and three- oscillator systems. The all-to-all Arnold tongue did not decrease significantly when going from a three to a four oscillator system. The Arnold tongue for chain systems showed a pattern of a geometric series. These are patterns which could be investigated for N-oscillators.

The classical Arnold tongues were shown to be good estimates for when synchronisation is expected to occur in the equivalent quantum system. For the chain system further analysis was done into how the strength of synchronisation changed between oscillators beyond just the first two, and how the synchronisation behaviour changed when the frequency difference was constant between each oscillator from 1 to 4. The synchronisation strength weakened as the distance between two oscillators was increased. Having the frequency difference between oscillators (1,2), (2,3) and (3,4) be a constant value led to a quantum Arnold tongue that more closely resembled the classical Arnold tongue. To determine the quantum Arnold tongues, two different synchronisation measures were used. The first measure was the complex-valued correlator between two oscillators which has frequently been used previously. The second measure was the relative entropy of coherence. In the case of quantum van der Pol oscillators this represented the relative entropy of synchronisation due the diagonal limit cycle of the quantum van der Pol oscillator. The relative entropy was also found to be a good measure for when synchronisation occurred. As opposed to the complex-valued correlator, the relative entropy of synchronisation takes into account the state of the system as a whole, as opposed to being a measure of synchronisation between two oscillators. As such, this would be a better measure for systems of more than two oscillators.

In order to understand the synchronisation of quantum van der Pol oscillators, one must first understand how damping can be incorporated into quantum systems, as the van der Pol oscillator involves negative and non-linear damping. This thesis discusses the problems faced in the ad-hoc approach of including damping via the equation of motion, and how damping can be successfully incorporated into the system by letting the system interact with a reservoir which is subsequently traced out. An equation very close to the master equation for the quantum van der Pol oscillator commonly studied [3][4][7][16] is reproduced, however this equation still retains a linear damping term that is not present for the quantum van der Pol oscillator.

6.2. Future research

Further research could investigate the synchronisation behaviour in systems containing 5 quantum van der Pol oscillators, of which there are 21 different arrangements. Due to how many different arrangements there

are, such an analysis will be computationally intensive. Systems that are generalisable to N oscillators such as the tree, chain, loop and all-to-all coupled systems would be a better goal as they are most comparable to the same type of systems with more or fewer oscillators. A relationship between the number of oscillators and the size of the Arnold tongue could then be determined, and subsequently compared to the quantum regime. Furthermore, the effect of varying the coupling strength between oscillators would also be interesting to investigate.

The relative entropy of coherence was appropriate as a measure of synchronisation for coupled quantum van der Pol oscillators. Due to this measure incorporating the entire system rather than only the correlation between two oscillators, this could be used for larger systems. It is important to remember that the measure as it is presented in this thesis is only applicable to systems which when uncoupled or undriven, would have diagonal limit cycles. Alternatively, the correlation coefficients between each oscillator could be averaged to determine the strength of the synchronisation present in the system as a whole, however it is uncertain if this would give a good measure.

A more in-depth investigation into the derivation of a master equation may allow one to obtain the master equation for the quantum van der Pol oscillator without having to exclude the linear damping term. The assumption in this derivation that the pump mode's reservoir had a mean photon number of zero could be left out, allowing an alternative master equation to be derived.

Bibliography

[1] Arkady Pikovsky, Michael Rosenblum, and Jürgen Kurths. *Synchronization: A Universal Concept in Nonlinear Sciences*. Cambridge Nonlinear Science Series. Cambridge University Press, 2001.

[2] Berislav Buca, Cameron Booker, and Dieter Jaksch. Algebraic theory of quantum synchronization and limit cycles under dissipation. *SciPost Physics*, 12(3):097, 2022.

[3] Tony E Lee and HR Sadeghpour. Quantum synchronization of quantum van der Pol oscillators with trapped ions. *Physical review letters*, 111(23):234101, 2013.

[4] Tony E. Lee, Ching-Kit Chan, and Shenshen Wang. Entanglement tongue and quantum synchronization of disordered oscillators. *Phys. Rev. E*, 89:022913, Feb 2014.

[5] Tim Klijnjan. Synchronisation along quantum trajectories of three coupled vdp oscillators. Bachelor's thesis, TU Delft, Jan 2021.

[6] Paweł Kurzyński. Synchronizing the simplest classical system and then quantizing it. *Phys. Rev. Research*, 2:033289, Aug 2020.

[7] Stefan Walter, Andreas Nunnenkamp, and Christoph Bruder. Quantum synchronization of a driven self-sustained oscillator. *Physical Review Letters*, 112(9), Mar 2014.

[8] De Voorhoede. Bloch sphere. https://www.quantum-inspire.com/kbase/bloch-sphere/.

[9] David J Griffiths and Darrell F Schroeter. *Introduction to quantum mechanics*. Cambridge University press, 2018.

[10] Howard J Carmichael. *Statistical methods in quantum optics 1: master equations and Fokker-Planck equations*, volume 1. Springer Science & Business Media, 1999.

[11] Tirth Shah, Rohitashwa Chattopadhyay, Kedar Vaidya, and Sagar Chakraborty. Conservative perturbation theory for nonconservative systems. *Phys. Rev. E*, 92:062927, Dec 2015.

[12] Ulf Leonhardt. *Essential quantum optics: from quantum measurements to black holes*. Cambridge University Press, 2010.

[13] Howard J Carmichael. *Statistical methods in quantum optics 2: Non-classical fields*. Springer Science & Business Media, 2009.

[14] Stefan Walter, Andreas Nunnenkamp, and Christoph Bruder. Quantum synchronization of two van der Pol oscillators. *Annalen der Physik*, 527(1-2):131–138, 2015.

[15] Lior Ben Arosh, MC Cross, and Ron Lifshitz. Quantum limit cycles and the Rayleigh and van der Pol oscillators. *Physical Review Research*, 3(1):013130, 2021.

[16] Najmeh Es'haqi-Sani, Gonzalo Manzano, Roberta Zambrini, and Rosario Fazio. Synchronization along quantum trajectories. *Phys. Rev. Research*, 2:023101, Apr 2020.

[17] Talitha Weiss, Andreas Kronwald, and Florian Marquardt. Noise-induced transitions in optomechanical synchronization. *New Journal of Physics*, 18(1):013043, 2016.

[18] Noufal Jaseem, Michal Hajdušek, Parvinder Solanki, Leong-Chuan Kwek, Rosario Fazio, and Sai Vinjanampathy. Generalized measure of quantum synchronization. *Physical Review Research*, 2(4):043287, 2020.

[19] J.R. Johansson, P.D. Nation, and Franco Nori. QuTiP: An open-source Python framework for the dynamics of open quantum systems. *Computer Physics Communications*, 183(8):1760–1772, Aug 2012.

[20] Code used for the figures and results of this thesis. https://github.com/wiggert9/Quantumsynchronisation.

A

Appendix

A.1. Amplitude equation

Equations (2.9), (2.12), (2.10) and (2.11) are first repeated below:

$$x(t) = \frac{1}{2}(Ae^{i\omega t} + A^* e^{-i\omega t}), \tag{A.1}$$

$$y(t) = \frac{1}{2}(i\omega Ae^{i\omega t} - i\omega A^* e^{-i\omega t}), \tag{A.2}$$

$$\dot{x} = y, \tag{A.3}$$

$$\dot{y} = -\omega^2 x + \mu(1-\beta x^2)\dot{x}. \tag{A.4}$$

Inserting equations (A.1) and (A.2) into equation (A.3) gives

$$\frac{1}{2}(i\omega Ae^{i\omega t} + \dot{A}e^{i\omega t} - i\omega A^* e^{-i\omega t} + \dot{A}^* e^{-i\omega t}) =) = \frac{1}{2}(i\omega Ae^{i\omega t} - i\omega A^* e^{-i\omega t}),$$

$$\implies \dot{A}e^{i\omega t} + \dot{A}^* e^{-i\omega t} = 0. \tag{A.5}$$

Then resolving for $\dot{y}$ and inserting into equation (A.4) leads to

$$\begin{aligned}
\dot{y} &= \frac{1}{2}(-\omega^2 Ae^{i\omega t} + i\omega\dot{A}(t)e^{i\omega t} - \omega^2 A^* e^{-i\omega t} - i\omega\dot{A}^* e^{-i\omega t}) \\
&= -\omega^2 x + i\omega\dot{A}e^{i\omega t} \\
\implies & i\omega\dot{A}e^{i\omega t} = \mu(1-\beta x^2)\dot{x} \\
\implies & \dot{A} = \frac{e^{-i\omega t}}{i\omega}(\mu(1-\beta x^2)\dot{x})
\end{aligned} \tag{A.6}$$

Inserting the equations for x into the r.h.s gives:

$$\begin{aligned}
\dot{A} &= \frac{e^{-i\omega t}}{i\omega}\left[\frac{\mu}{2}(i\omega Ae^{i\omega t} - i\omega A^* e^{-i\omega t})\left(1 - \frac{\beta}{4}(A^2 e^{2i\omega t} + 2AA^* + A^{*2} e^{-2i\omega t})\right)\right] \\
&= \frac{\mu}{2}\left[(A - A^* e^{-2i\omega t}) - \frac{\beta}{4}\left(A^2 e^{2i\omega t} + 2A^2 A^* + AA^{*2} e^{-2i\omega t} - A^2 A^* - 2AA^{*2} e^{-2i\omega t} + A^{*3} e^{-4i\omega t}\right)\right]
\end{aligned} \tag{A.7}$$

Then performing the averaging by leaving out all the oscillating terms gives:

$$\dot{A} = \frac{\mu}{2}\left[A - \frac{\beta}{4}A^2 A^*\right] \tag{A.8}$$

$$= \frac{\mu}{2}A - \frac{\mu\beta}{8}|A|^2 A \tag{A.9}$$

which is the amplitude equation for the van der Pol oscillator as desired.

A.2. Rotating wave approximation

We start with the following equation representing the coupling between the two oscillators.

$$\begin{aligned}\hat{x}_1\hat{x}_2 &= \frac{\hbar}{2\sqrt{m_1 m_2\omega_1\omega_2}}(\hat{a}_1 + \hat{a}^\dagger{}_1)(\hat{a}_2 + \hat{a}^\dagger{}_2),\\ &= \frac{\hbar}{2\sqrt{m_1 m_2\omega_1\omega_2}}(\hat{a}_1\hat{a}_2 + \hat{a}_1^\dagger\hat{a}_2 + \hat{a}_1\hat{a}_2^\dagger + \hat{a}_1^\dagger\hat{a}_2^\dagger).\end{aligned} \tag{A.10}$$

When the transformation is made to the interaction picture, with $H_0 = \hbar\omega_1\hat{a}_1^\dagger\hat{a}_1 + \hbar\omega_2\hat{a}_2^\dagger\hat{a}_2$ (as will be done in the derivation), the operators $\hat{a}_1$ and $\hat{a}_2$ transform to

$$\hat{a}_{1,I}(t) = e^{i\omega_1\hat{a}_1^\dagger\hat{a}_1 t}\hat{a}_1 e^{-i\omega_1\hat{a}_1^\dagger\hat{a}_1 t}, \tag{A.11}$$

$$\hat{a}_{2,I}(t) = e^{i\omega_2\hat{a}_2^\dagger\hat{a}_2 t}\hat{a}_2 e^{-i\omega_2\hat{a}_2^\dagger\hat{a}_2 t}. \tag{A.12}$$

where the fact that operators acting solely on the first oscillator commute with operators acting solely on the second oscillator is used (so terms including $\hat{a}_2$ cancel out in the equation for $\hat{a}_1$.

These operators can be evaluated. Taking the derivative of Equation (A.11) leads to

$$\begin{aligned}\frac{d}{dt}\hat{a}_{1,I}(t) &= i\omega_1\hat{a}_1^\dagger\hat{a}_1\left(e^{i\omega_1\hat{a}_1^\dagger\hat{a}_1 t}\hat{a}_1 e^{-i\omega_1\hat{a}_1^\dagger\hat{a}_1 t}\right) - \left(e^{i\omega_1\hat{a}_1^\dagger\hat{a}_1 t}\hat{a}_1\right)i\omega_1\hat{a}_1^\dagger\hat{a}_1\left(e^{-i\omega_1\hat{a}_1^\dagger\hat{a}_1 t}\right)\\ &= e^{i\omega_1\hat{a}_1^\dagger\hat{a}_1 t}\left[i\omega_1\hat{a}_1^\dagger\hat{a}_1, \hat{a}_1\right]e^{-i\omega_1\hat{a}_1^\dagger\hat{a}_1 t}.\end{aligned} \tag{A.13}$$

The commutation relations evaluates as follows:

$$\begin{aligned}\left[i\omega_1\hat{a}_1^\dagger\hat{a}_1, \hat{a}_1\right] &= i\omega_1\left(\hat{a}_1^\dagger\hat{a}_1\hat{a}_1 - \hat{a}_1\hat{a}_1^\dagger\hat{a}_1\right)\\ &= i\omega_1(-\hat{a}_1),\end{aligned} \tag{A.14}$$

where the commutation relation in Equation (3.20) is used.

Substituting this into Equation (A.13) leads to

$$\frac{d}{dt}\hat{a}_{1,I}(t) = e^{i\omega_1\hat{a}_1^\dagger\hat{a}_1 t}(-i\omega_1\hat{a}_1)e^{-i\omega_1\hat{a}_1^\dagger\hat{a}_1 t} = -i\omega_1\hat{a}_{1,I}(t). \tag{A.15}$$

This differential equation has the following solution:

$$\hat{a}_{1,I}(t) = \hat{a}_1 e^{-i\omega_1 t}, \tag{A.16}$$

$$\hat{a}_{2,I}(t) = \hat{a}_2 e^{-i\omega_2 t}, \tag{A.17}$$

where the solution for $\hat{a}_{2,I}$ can be derived in the same way. The creation operators $\hat{a}_i^\dagger$ are the complex conjugates of these.

Substituting this into Equation (3.31) leads to

$$\hat{x}_1\hat{x}_2 = \frac{\hbar}{2\sqrt{m_1 m_2\omega_1\omega_2}}\left(\hat{a}_1\hat{a}_2 e^{-it(\omega_1+\omega_2)} + \hat{a}_1^\dagger\hat{a}_2 e^{-it(-\omega_1+\omega_2)} + \hat{a}_1\hat{a}_2^\dagger e^{-it(\omega_1-\omega_2)} + \hat{a}_1^\dagger\hat{a}_2^\dagger e^{it(\omega_1+\omega_2)}\right). \tag{A.18}$$

Now the rotating wave approximation can be made. The first and fourth terms in Equation (A.18) both have a summation of the frequencies of the two oscillators, meaning that these terms are fast oscillating. The rotating wave approximation neglects the fast oscillating terms, therefore only the second and third term (which are assumed to be slowly oscillating as the two frequencies are subtracted from one another) are left in our Hamiltonian.

This means that after making the rotating wave approximation, the coupling can be written as

$$C \cdot \left(\hat{a}_1^\dagger \hat{a}_2 e^{-it(-\omega_1+\omega_2)} + \hat{a}_1 \hat{a}_2^\dagger e^{-it(\omega_1-\omega_2)} \right), \tag{A.19}$$

with C a constant. Transforming this back to the Schrödinger picture leads to the following term in the Hamiltonian

$$C \cdot (\hat{a}_1^\dagger \hat{a}_2 + \hat{a}_1 \hat{a}_2^\dagger). \tag{A.20}$$

A.3. Superoperators in interaction picture

A new superoperator $\mathcal{S}'$ can be defined by

$$\mathcal{S}' = e^{-\mathcal{L}} \mathcal{S} e^{\mathcal{L}} \tag{A.21}$$

where $\mathcal{L}$ is the superoperator defining the transformation into the interaction picture(or another picture). This new superoperator obeys the equation of motion

$$\frac{dS'}{dt} = [S', \mathcal{L}] \tag{A.22}$$

This equation can be solved to find the superoperator in the interaction picture.
If $S = (b\cdot)$,$\mathcal{L} = \frac{\gamma_p}{2}(2b\cdot b^\dagger - b^\dagger b \cdot - \cdot b^\dagger b)$ then,

$$\frac{d(b\cdot)'}{dt} = \left[(b\cdot)', \frac{\gamma_p}{2} \left(2(b\cdot b^\dagger)' - (b^\dagger b\cdot)' - (\cdot b^\dagger b)' \right) \right] \tag{A.23}$$

$$= \frac{\gamma_p}{2} \left[2(bb\cdot b^\dagger)' - (bb^\dagger b\cdot)' - (b\cdot b^\dagger b)' - \left(2(bb\cdot b^\dagger)' - (b^\dagger bb\cdot)' - (b\cdot b^\dagger b)' \right) \right] \tag{A.24}$$

$$= -\frac{\gamma_p}{2}([b, b^\dagger] b\cdot)' = -\frac{\gamma_p}{2}(b\cdot)' \tag{A.25}$$

Using the initial value, $(b\cdot)'(t=0) = (b\cdot)$, this equation can be solved giving

$$(b\cdot)' = e^{-\mathcal{L}}(b\cdot)e^{\mathcal{L}} = e^{-\frac{\gamma_p}{2}t}(b\cdot) \tag{A.26}$$

This gives Equation (3.100). Equation (3.101) is slightly more difficult:

$$\frac{d(b^\dagger\cdot)'}{dt} = \left[(b^\dagger\cdot)', \frac{\gamma_p}{2} \left(2(b\cdot b^\dagger)' - (b^\dagger b\cdot)' - (\cdot b^\dagger b)' \right) \right] \tag{A.27}$$

$$= \frac{\gamma_p}{2} \left[2(b^\dagger b\cdot b^\dagger)' - (b^\dagger b^\dagger b\cdot)' - (b^\dagger\cdot b^\dagger b)' - \left(2(bb^\dagger\cdot b^\dagger)' - (b^\dagger bb^\dagger\cdot)' - (b^\dagger\cdot b^\dagger b)' \right) \right] \tag{A.28}$$

$$= \frac{\gamma_p}{2} \left[-2(\cdot b^\dagger)' + (b^\dagger\cdot)' \right] \tag{A.29}$$

Taking the conjugate of Equation (A.26), evaluates the first term, leading to the following first order differential equation

$$\frac{d(b^\dagger\cdot)'}{dt} - \frac{\gamma_p}{2}(b^\dagger\cdot)' = -e^{-\frac{\gamma_p}{2}t}(\cdot b^\dagger) \tag{A.30}$$

Using the initial value $(b^\dagger\cdot)'(t=0) = (b^\dagger\cdot)$, this is solvable with standard methods, leading to Equation (3.101):

$$(b^\dagger)' = e^{-\mathcal{L}t}(b^\dagger)e^{\mathcal{L}t} = e^{\frac{\gamma_p}{2}t}(b^\dagger\cdot) + \left(e^{-\frac{\gamma_p}{2}t} - e^{\frac{\gamma_p}{2}t} \right)(\cdot b^\dagger) \tag{A.31}$$